nature genetics

Article

https://doi.org/10.1038/s41588-022-01240-7

Antagonistic control of seed dormancy in rice by two bHLH transcription factors

Received: 5 May 2022

Accepted: 24 October 2022

Published online: 05 December 2022

Check for updates

Fan Xu[1,2,9], Jiuyou Tang[1,9], Shengxing Wang[3,9], Xi Cheng[1,2,9], Hongru Wang[4], Shujun Ou[5], Shaopei Gao[1], Boshu Li[3], Yangwen Qian[6], Caixia Gao[3,7] ✉ & Chengcai Chu[1,8] ✉

Preharvest sprouting (PHS) due to lack of seed dormancy seriously threatens crop production worldwide. As a complex quantitative trait, breeding of crop cultivars with suitable seed dormancy is hindered by limited useful regulatory genes. Here by repeatable phenotypic characterization of fixed recombinant individuals, we report a quantitative genetic locus, *Seed Dormancy 6* (*SD6*), from *aus*-type rice, encoding a basic helix-loop-helix (bHLH) transcription factor, which underlies the natural variation of seed dormancy. *SD6* and another bHLH factor inducer of C-repeat binding factors expression 2 (ICE2) function antagonistically in controlling seed dormancy by directly regulating the ABA catabolism gene *ABA8OX3*, and indirectly regulating the ABA biosynthesis gene *NCED2* via OsbHLH048, in a temperature-dependent manner. The weak-dormancy allele of *SD6* is common in cultivated rice but undergoes negative selection in wild rice. Notably, by genome editing *SD6* and its wheat homologs, we demonstrated that *SD6* is a useful breeding target for alleviating PHS in cereals under field conditions.

Seed dormancy is a strategy of plants that enables seeds to remain quiescent until conditions become favorable for germination[1]. Seed dormancy affects seed dispersal and influences the location and timing of plant growth, and thus is under strong selection in natural plant populations[2]. Adequate dormancy keeps seeds in a quiescent state in the field[3], while weak dormancy ensures a higher and more uniform emergence rate after sowing[4,5]. However, weak seed dormancy also leads to unwanted early germination of freshly matured seeds on the mother plants, called preharvest sprouting (PHS). For a long time, PHS in cereals including rice and wheat has become a serious problem worldwide, leading to reduced grain quality and yield[6–9].

Seed dormancy and germination are complex agronomic traits controlled by many quantitative genetic loci (QTLs)[6]. The Gramene QTL database documents 164 rice QTLs associated with seed dormancy or germination (http://www.gramene.org). These QTLs have been reported from a variety of sources, including cultivated rice[10–15], wild rice[16–19] and weedy rice[20–23], but only few genes have so far been characterized at the molecular level. The transcription factor (TF) *Sdr4* is a global regulator of seed maturation regulated by OsVP1 (ref. [24]). *qSD7-1* has been traced to the pleiotropic locus *Rc* and found to control seed dormancy by regulating the ABA biosynthesis pathway[25]. *qSD1-2* was identified as the GA synthesis gene *OsGA20ox2* that may induce primary

[1]State Key Laboratory of Plant Genomics, Institute of Genetics and Developmental Biology, Innovation Academy for Seed Design, Chinese Academy of Sciences, Beijing, China. [2]Key Laboratory of Biotechnology and Crop Quality Improvement, Ministry of Agriculture/Biotechnology Research Center, Southwest University, Chongqing, China. [3]State Key Laboratory of Plant Cell and Chromosome Engineering, Center for Genome Editing, Institute of Genetics and Developmental Biology, Innovation Academy for Seed Design, Chinese Academy of Sciences, Beijing, China. [4]Department of Integrative Biology, University of California Berkeley, Berkeley, CA, USA. [5]Department of Ecology, Evolution, and Organismal Biology, Iowa State University, Ames, IA, USA. [6]Biogle Genome Editing Center, Changzhou, China. [7]College of Advanced Agricultural Sciences, University of Chinese Academy of Sciences, Beijing, China. [8]Guangdong Laboratory for Lingnan Modern Agriculture, State Key Laboratory for Conservation and Utilization of Subtropical Agro-Bioresources, College of Agriculture, South China Agricultural University, Guangzhou, China. [9]These authors contributed equally: Fan Xu, Jiuyou Tang, Shengxing Wang, and Xi Cheng. ✉e-mail: cxgao@genetics.ac.cn; ccchu@genetics.ac.cn

dormancy by a GA-regulated dehydration mechanism[26]. *qSd1-1* encodes OsDOG1L-3, a protein homologous to *Arabidopsis* DOG1, contributing to seed dormancy establishment in rice[27]. Recently, we identified the *G* gene, which influences seed dormancy via an action on ABA biosynthesis, and has been subjected to parallel selection in several crop families[6].

Here we report the successful dissection of the complex agronomic traits, seed dormancy, into an important QTL, *Seed Dormancy 6* (*SD6*). *SD6* along with another basic helix-loop-helix (bHLH) TF, inducer of C-repeat binding factors expression 2 (ICE2) antagonistically balance the expression of the ABA catabolism gene *ABA8OX3* and biosynthesis gene *NCED2* to control rice seed dormancy by responding to temperature signals. We further confirmed that *SD6* is functionally conserved in rice and wheat and could be a powerful target for improving PHS resistance in cereals under field conditions.

Results

Natural alleles of *SD6* confer PHS resistance

To identify genes underlying the natural variations in rice seed dormancy, we screened several chromosome single-segment substitution lines (CSSSLs) derived from a cross between weak-dormancy cultivar Nipponbare and strong-dormancy cultivar Kasalath for the previously reported stable QTL regions. Germination experiment of fresh seeds indicated that five CSSSLs exhibited stronger seed dormancy than Nipponbare. One of these lines, Q27, was selected for further analysis, in which a segment on chromosome 6 of Kasalath containing reported seed dormancy QTLs[16,28] has been introgressed into the Nipponbare background. Freshly harvested seeds of Q27 exhibited dormancy close to that of Kasalath (Fig. 1a–c and Extended Data Fig. 1), indicating that the substituted segment contained a seed dormancy locus with large effect, and was therefore termed *SD6*. For fine-mapping of *SD6*, an F_2 segregated population was generated by backcrossing Q27 to Nipponbare to firstly screen fixed homozygous recombinant individuals using molecular markers covering the target region (Fig. 1d). Finally, progeny phenotyping of fixed homozygous recombinant individuals narrowed *SD6* to an ~20-kb region, which contains five predicted ORFs (Fig. 1f). Among them, only *LOC_Os06g06900* and *LOC_Os06g06910* were expressed in seeds (Supplementary Table 1). Sequence comparison between Nipponbare and Kasalath demonstrated that there are no SNPs in *LOC_Os06g06910* but six SNPs are present in *LOC_Os06g06900*—SNP1 (+548 A/C), SNP2 (+1349 G/A) and SNP4 (+2236 A/G) are located in the intron; SNP5 (+2387 T/C) leads to a synonymous amino acid substitution, while SNP3 (+1857 T/C) and SNP6 (+2409 A/T) result in nonsynonymous changes, corresponding Valine (V) to Alanine (A) and Serine (S) to Cysteine (C), respectively (Fig. 1f and Extended Data Fig. 2).

We developed a near-isogenic line (NIL) of *SD6* (NIL-SD6) with the ~20-kb Kasalath segment between markers S7 and S8 in the Nipponbare background (Fig. 1e). Seeds in freshly harvested mature panicles of NIL-SD6 exhibited strong-dormancy compared with that of Nipponbare (Fig. 1g,h). Moreover, seeds in freshly harvested mature panicles of *LOC_Os06g06900* knockout mutants (*sd6-1* and *sd6-3*) had a seed germination percentage as low as 3% after 7-d imbibition, in sharp contrast to that of more than 85% for Zhonghua11 (ZH11), whereas germination percentages of *LOC_Os06g06900* overexpression lines (SO2-7 and SO3-6) reached 85% after 5-d imbibition and that of ZH11 was 7% (Fig. 1i–l and Extended Data Fig. 3a,b). Once seed dormancy was released following a one-week 45 °C treatment, both knockout mutants and overexpression lines exhibited comparable germination performance to ZH11 (Extended Data Fig. 3c). These results confirmed that *LOC_Os06g06900* is the causal gene underlying the *SD6* locus and functions as a negative regulator of seed dormancy rather than after-ripening seed germination. The *sd6* mutants also displayed significantly increased grain numbers per spike (Supplementary Table 2), which makes *SD6* a good candidate for breeding cultivars with both PHS resistance and increased yield. Additionally, no obvious expression difference of *SD6* between Nipponbare and NIL-SD6 seeds was detected (Extended Data Fig. 3d), suggesting that functional differences between Nipponbare and Kasalath alleles of *SD6* may not be attributed to the variations in their promoters.

SD6 and *ICE2* antagonistically regulate rice seed dormancy

SD6 encodes a putative bHLH TF. Dimerization of bHLH TFs is crucial for their DNA-binding activity[29]. Using SD6 as a bait, we screened for SD6-interaction proteins by yeast two-hybrid (Y2H) and found another bHLH TF, ICE2, interacts with SD6 (Fig. 2a and Supplementary Table 3). Interestingly, although *SD6* and *ICE2* were both expressed in seeds, the level of *SD6* transcripts decreased with seed development, whereas that of *ICE2* transcripts increased at a higher order of magnitude, implying different roles of *SD6* and *ICE2* in regulating seed dormancy (Fig. 2b). Subcellular localization analyses showed that SD6 and ICE2 were both localized in the nucleus (Fig. 2c). Homodimerization of SD6 and ICE2 or heterodimerization between them was demonstrated by bimolecular fluorescence complementation (BiFC) experiments, and the interaction between SD6 and ICE2 was further validated by pull-down assays (Fig. 2d,e).

Knockout of *ICE2* led to significantly enhanced susceptibility to PHS compared to its wild-type ZH11, whereas the seeds in freshly harvested mature panicles of the *ICE2*-overexpressing lines, IO1-2 and IO1-8, had a strong-dormancy phenotype (Fig. 2f–i and Extended Data Fig. 3e–g). These results indicated that ICE2 has a role opposite to SD6 in seed dormancy. Moreover, unlike the *sd6* mutants, the *ice2* mutants had reduced grain numbers per spike (Supplementary Table 2).

SD6 and ICE2 target *ABA8OX3* to modulate seed dormancy

The role of ABA in seed dormancy onset has been well-documented by numerous genetic and physiological studies[30–34]. Thus, we detected the ABA contents in the seeds of *sd6* and *ice2* mutants at 21–25 days after pollination (DAP), the stage at which rice seeds normally enter dormancy[35]. The ABA contents of NIL-SD6, *sd6-1*, *sd6-3*, IO1-2 and IO1-8 seeds were significantly higher than that of their corresponding control seeds, whereas the ABA contents of *ice2-1*, *ice2-2*, SO2-7 and SO3-6 seeds were lower than that of ZH11 seeds (Fig. 3a and Extended Data Fig. 4). Furthermore, the major ABA biosynthesis gene, *NCED2*, expressed in seeds at 21–25 DAP, is significantly upregulated in NIL-SD6, *sd6-1* and *sd6-3* and downregulated in *ice2-1* and *ice2-2* compared to their wild-type controls. Conversely, the major ABA catabolism gene, *ABA8OX3*, expressed in seeds at 21–25 DAP, shows an opposite regulation trend to *NCED2* by SD6 and ICE2. These results suggest that SD6 and ICE2 control ABA content in seeds by antagonistically regulating the expression of ABA metabolism genes (Fig. 3b,c).

The bHLH-type TFs often bind to E-box (CANNTG) or G-box (CACGTG) motifs present in the promoters of target genes[36,37]. We identified multiple G- or E-boxes in the promoters and 3′-UTR regions of *NCED2* and *ABA8OX3* (Fig. 3d). Using yeast-one-hybrid (Y1H), we verified that SD6 and ICE2 specifically bind artificial sequences with triple G- and E-box motifs, respectively (Extended Data Fig. 5a). Chromatin immunoprecipitation (ChIP)-qPCR assays further showed enrichment of only *ABA8OX3* G-box-specific amplicons for SD6 and only *ABA8OX3* E-box-specific amplicons for ICE2, indicating that *ABA8OX3* is the common target of SD6 and ICE2 (Fig. 3e,f). Using a luciferase (LUC) reporter system, we further showed that SD6 and ICE2 bound to roughly 2.5 kb promoter of *ABA8OX3*, which contains the site 1 G-box and site 3 E-boxes as indicated in Fig. 3d. Moreover, SD6 activated the expression of *ABA8OX3*, whereas ICE2 inhibited it (Fig. 3g), consistent with the expression level of *ABA8OX3* in the seeds of *sd6* and *ice2* mutants (Fig. 3c). When *SD6, ICE2* and the reporter pABA8OX3-LUC, which contains the 2.5 kb promoter region of *ABA8OX3*, were co-expressed in rice protoplasts, the expression of LUC was gradually reduced with increasing levels of *ICE2* (Fig. 3h). We further generated the reporter vectors pA8OX3-P1-LUC, which contains an intact G-box but mutated

https://doi.org/10.1038/s41588-022-01240-7

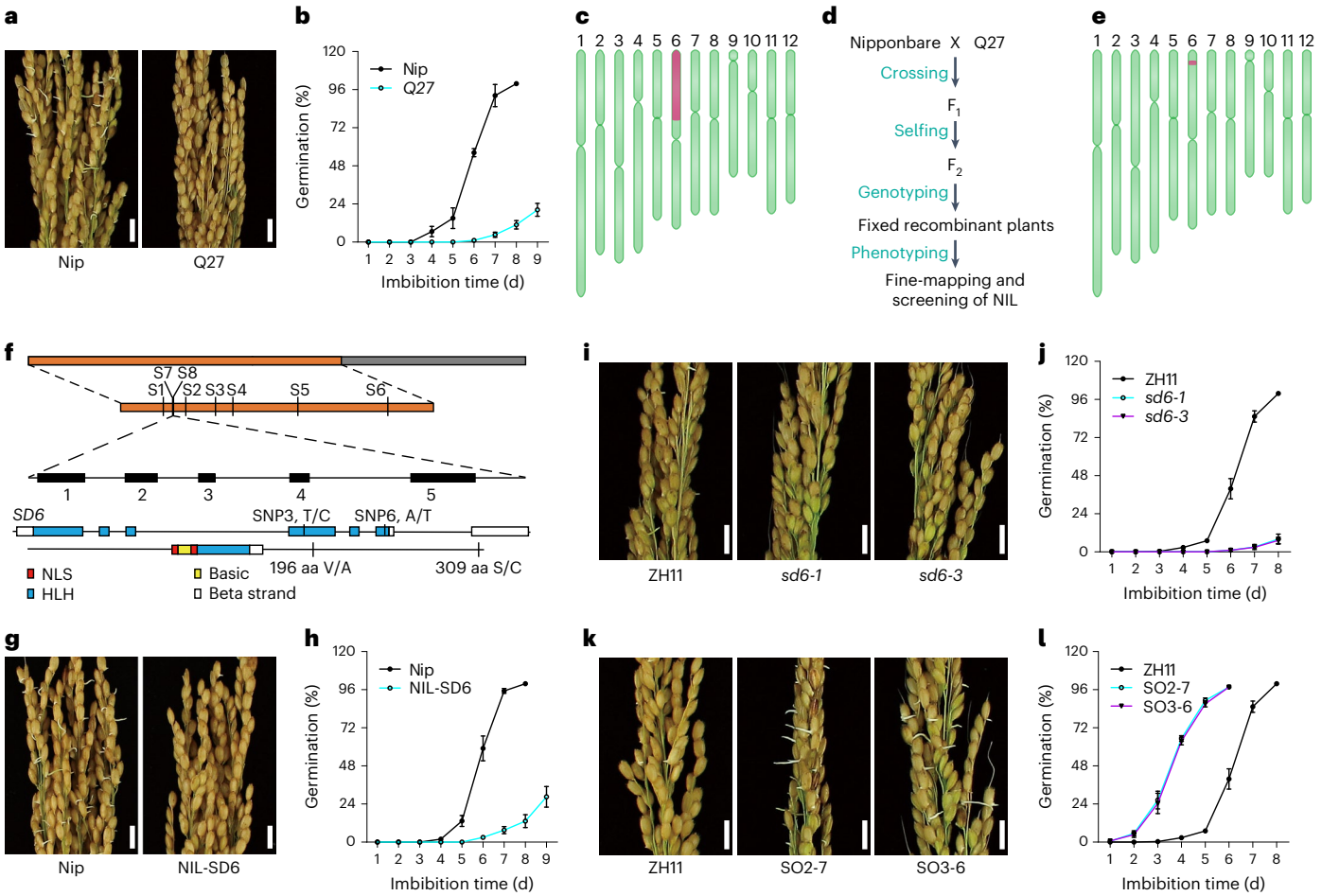

Fig. 1 | Identification of *SD6*. **a**, Germination performance of seeds in freshly harvested mature panicles of CSSSL Q27. Scale bar, 1 cm. **b**, Time-course germination percentage of seeds in freshly collected mature panicles of CSSSL Q27. **c**, Graphical genotype of CSSSL (Q27). Green region, genomic region from Nipponbare; red region, genomic region from Kasalath. **d**, Schematic representation to generate F_2 population from Q27 × Nipponbare. **e**, Schematic representation of NIL-SD6. Green region, genomic region from Nipponbare; red region, genomic region from Kasalath. **f**, Map-based cloning of *SD6*. *SD6* was delimited to a genomic region containing five predicted ORFs (upper panel). Middle panel: the exon–intron structure of *SD6* gene and the location of nonsynonymous substitutions. Bottom panel: characteristic structure and amino acid substitutions of SD6 protein. NLS, nuclear localization signal. **g**, Germination performance of seeds in freshly harvested mature panicles of NIL-SD6. Scale bar, 1 cm. **h**, Time-course germination percentage of seeds in freshly collected mature panicles of NIL-SD6. **i**,**k**, Germination performance of seeds in freshly harvested mature panicles of *sd6* mutants (**i**) and *SD6* overexpression plants (**k**). Scale bar, 1 cm. **j**,**l**, Time-course germination percentage of seeds in freshly collected mature panicles of *sd6* mutants (**j**) and *SD6* overexpression plants (**l**). Each germination test was repeated with four panicle replicates. Photographs were taken after 6-d imbibition for Nipponbare background plants and 5-d imbibition for ZH11 background plants. Data are presented as mean ± s.d.

E-boxes in the *ABA8OX3* promoter, and pA8OX3-P2-LUC, which harbors the 1.9 kb *ABA8OX3* promoter with intact E-boxes but no G-box, to avoid any potential competitive binding by SD6 and ICE2 to the same promoter position due to the presence of both E-box and G-box. When these two reporters were co-expressed with *SD6* and *ICE2*, respectively, pA8OX3-P1-triggered LUC expression was gradually reduced with increasing levels of ICE2; in contrast, pA8OX3-P2-triggered LUC expression was gradually increased with increasing levels of SD6, suggesting that the interaction between SD6 and ICE2 largely reduces their binding ability with their respective target motifs (Extended Data Fig. 6). The lower transcriptional activation activity of Kasalath-type $SD6^{Kasa}$ than that of Nipponbare-type ($SD6^{Nip}$) might explain the lower expression level of *ABA8OX3* (0.8-fold) and higher ABA content of NIL-SD6 compared with Nipponbare, and stronger dormancy of NIL-SD6 seeds. Moreover, the transcriptional activation activity of $SD6^{S309C}$ was similar to $SD6^{Nip}$, while $SD6^{V196A}$ exhibited similar transcriptional activation activity to $SD6^{Kasa}$, suggesting that the C-to-T mutation at SNP3 is the causal variant of *SD6* (Fig. 3g).

Additionally, independent *aba8ox3* mutant lines exhibited stronger seed dormancy than wild-type plants (Fig. 3i,j and Extended Data Fig. 7a,b), supporting the notion that changes in *ABA8OX3* expression observed in the *sd6* or *ice2* mutants lead to altered seed dormancy.

SD6 and ICE2 regulate *NCED2* in an indirect manner

Although significant changes in *NCED2* expression were observed in *sd6* and *ice2*, ChIP-qPCR assays failed to detect any SD6 or ICE2 binding to the *NCED2* promoter, suggesting that SD6 and ICE2 may regulate *NCED2* expression indirectly. AtbHLH57, a bHLH TF, positively regulates seed dormancy in *Arabidopsis* via directly binding to the promoter of *NCED6* and *NCED9* to elevate their expression[38], inspiring us to search for *AtbHLH57* homologs in rice to find any possible interactions between SD6/ICE2 and NCED2. Indeed, we identified significant changes in the expression of *LOC_Os02g52190*, one of the most homologous genes to *AtbHLH57* in rice, which has previously been named as *OsbHLH048* (ref. [39]), in both *sd6* and *ice2* mutants. *OsbHLH048* was sharply suppressed in the *sd6* seeds but significantly increased in *ice2* seeds (Fig. 4a),

https://doi.org/10.1038/s41588-022-01240-7

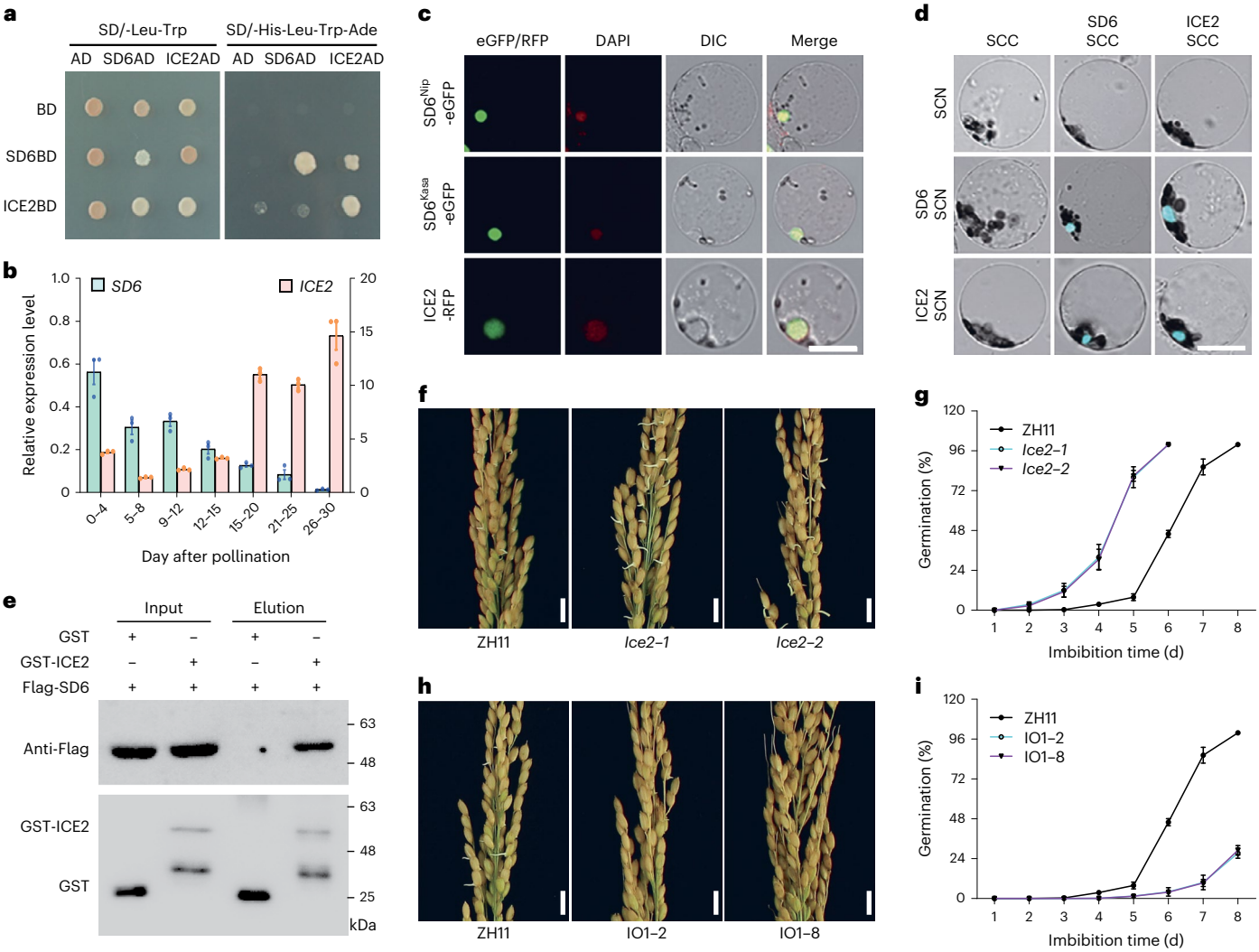

Fig. 2 | ICE2 interacting with SD6 positively regulates rice seed dormancy. **a**, The interaction between SD6 and ICE2 detected by Y2H assays. **b**, The expression patterns of *SD6* and *ICE2* in seeds detected by qRT-PCR. Each analysis was repeated with three biological replicates. Data are presented as mean ± s.d. **c**, Localization of SD6 and ICE2 in rice protoplasts. $SD6^{Nip}$ and $SD6^{Kasa}$ denote Nipponbare and Kasalath haplotypes of SD6, respectively. Scale bar, 10 μm. **d**, Visualization of the interactions between SCC merged proteins (SCC, SD6 SCC, and ICE2 SCC) and SCN merged proteins (SCN, SD6 SCN, and ICE2 SCN) detected by the BiFC assays in rice protoplasts. SCC and SCN represent C- and N-terminals of CFP protein, respectively. Scale bar, 10 μm. **e**, The interaction between SD6 and ICE2 detected by GST pull-down assays. Five micrograms of GST or GST-ICE2 coupled magnetic beads were used to pull down Flag-GFP or Flag-SD6 proteins from the transgenic plants. The experiment was repeated three times with similar results obtained. **f**,**h**, Germination performance of seeds in freshly harvested mature panicles of *ice2* mutants (**f**) and *ICE2* overexpression plants (**h**). Scale bar, 1 cm. **g**,**i**, Time-course germination percentage of seeds in freshly collected mature panicles of *ice2* mutants (**g**) and *ICE2* overexpression plants (**i**). Each germination test was repeated with four panicle replicates and photographs were taken after 5-d imbibition. Data are presented as mean ± s.d.

indicating that *OsbHLH048* may have contrasting functions to its homolog in *Arabidopsis*. Accordingly, ChIP-qPCR assays and transient transactivation assays showed that SD6 and ICE2 target the *OsbHLH048* promoter to regulate its expression (Fig. 4b,c).

We obtained two *osbhlh048* mutant lines from a CRISPR mutant library[40] (Extended Data Fig. 7e,f). Consistent with the expression changes in *sd6* and *ice2*, both *osbhlh048* lines showed increased seed dormancy compared to wild type (Fig. 4d,e), suggesting that *OsbHLH048* negatively regulates seed dormancy.

Intriguingly, an opposite regulatory relationship between *OsbHLH048* and the ABA synthesis gene *NCED2* was observed in rice. Specifically, the expression of *NCED2* was upregulated in *osbhlh048* seeds (Fig. 4f), and OsbHLH048 was able to inhibit the expression of an *NCED2* promoter-driven LUC reporter in rice protoplasts (Fig. 4h). ChIP-qPCR assays further confirmed that OsbHLH048 physically binds to the E-box motifs of the *NCED2* promoter (Fig. 4g). Together, these results revealed SD6/ICE2-OsbHLH048-NCED2 cascade in regulating rice seed dormancy.

Unlike metabolism-related genes, we did not observe SD6 or ICE2 binding to the promoter of either *ABI3* or *ABI5*, two important TFs in ABA signaling pathway[41] by ChIP-qPCR, and their expression was also not altered in the seeds of *sd6* and *ice2* (Extended Data Fig. 5b–f).

SD6 and ICE2 integrate temperature signaling

Temperature has a major effect on the strength of seed dormancy and seed sensitivity to environmental signals (such as light, nitrate, water potential, etc.)[42,43]. In *Arabidopsis*, AtICE1 and AtICE2, two homologs of ICE2 (Extended Data Fig. 8a), act as positive regulators of cold acclimation[44–49]. We examined the expression level of *SD6* and *ICE2* during seed germination at both room (25 °C) and low temperature (4 °C). *SD6* was significantly upregulated after 24-h imbibition at room temperature and slightly inhibited after 24-h imbibition at low temperature, whereas

https://doi.org/10.1038/s41588-022-01240-7

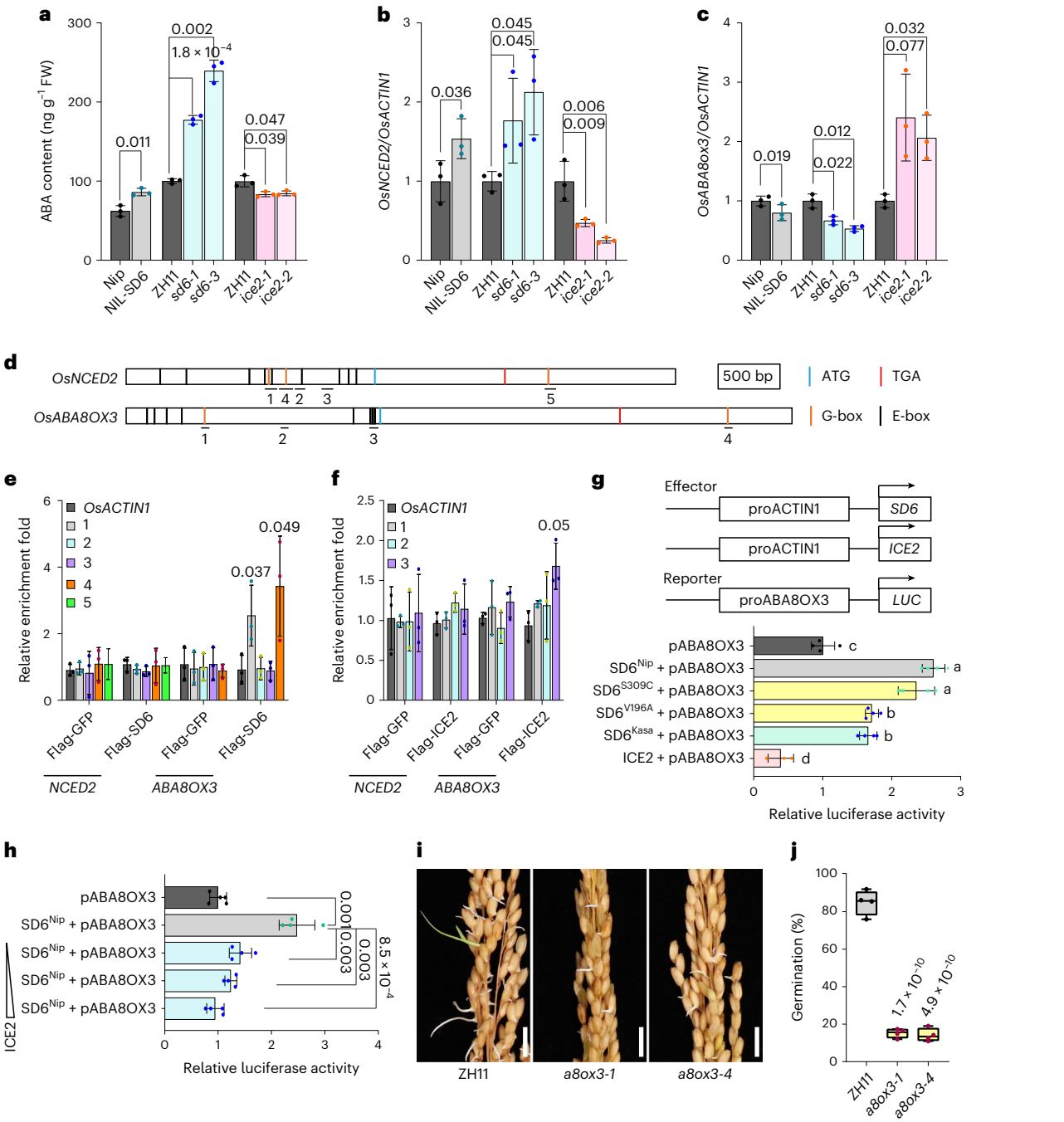

Fig. 3 | *ABA8OX3* is a direct target of SD6 and ICE2. a, The ABA content in freshly harvested 21–25 DAP seeds of Nipponbare, NIL-SD6, ZH11, *sd6* mutants and *ice2* mutants. **b**,**c**, The expression level of *NCED2* and *ABA8OX3* in freshly harvested 21–25 DAP seeds of Nipponbare, NIL-SD6, ZH11, *sd6* mutants and *ice2* mutants. **d**, Schematic representation of the indicated genes; vertical light blue bar represents the start codon ATG; vertical red bar represents the stop codon TGA; vertical orange bars represent G-box motifs; vertical gray bars represent E-box motifs; horizontal thin black lines represent amplicons assayed for SD6 and ICE2 binding. **e**,**f**, Relative ChIP-qPCR enrichment of the indicated promoter regions of *NCED2* and *ABA8OX3* for SD6 (**e**) and ICE2 (**f**). Flag-GFP was served as a negative control. Fragment of *OsACTIN1* gene body region was used as interval negative control. **g**, *ABA8OX3-LUC* expression in rice protoplasts cotransformed with $SD6^{Nip}$, $SD6^{S309C}$, $SD6^{V196A}$, $SD6^{Kasa}$ or *ICE2*. Statistical analysis was performed using one-way ANOVA. Different letters above the bars indicate a significant difference at $P < 0.05$. **h**, *ABA8OX3-LUC* expression in rice protoplasts cotransformed with $SD6^{Nip}$ and *ICE2*. **i**,**j**, Germination performance (**i**) and germination percentage (**j**) of seeds in freshly harvested 31–35 DAP panicles of *aba8ox3* mutants. Scale bar, 1 cm. Analysis in **a**–**c**, **e** and **f** was repeated with three biological replicates; *LUC* expression in **g** and **h** was repeated with four biological replicates. Germination test in **i** and **j** was repeated with four panicle replicates and photographs were taken after 7-d imbibition. Data are presented as mean ± s.d. for **a**–**c** and **e**–**h**. All *P* values are based on two-tailed Student's *t* tests; number marked for each data is the exact *P* value.

ICE2 was sharply downregulated after 12-h imbibition at room temperature and markedly increased after 24-h imbibition at low temperature (Fig. 5a,b). Furthermore, the expression level of *ABA8OX3* was lowest at the seed dormant phase (Fig. 5c), when *ICE2* was highly expressed and *SD6* was in low expression (Fig. 2b). Consistently, the expression of *ABA8OX3* showed a similar up-and-down change pattern to that of

https://doi.org/10.1038/s41588-022-01240-7

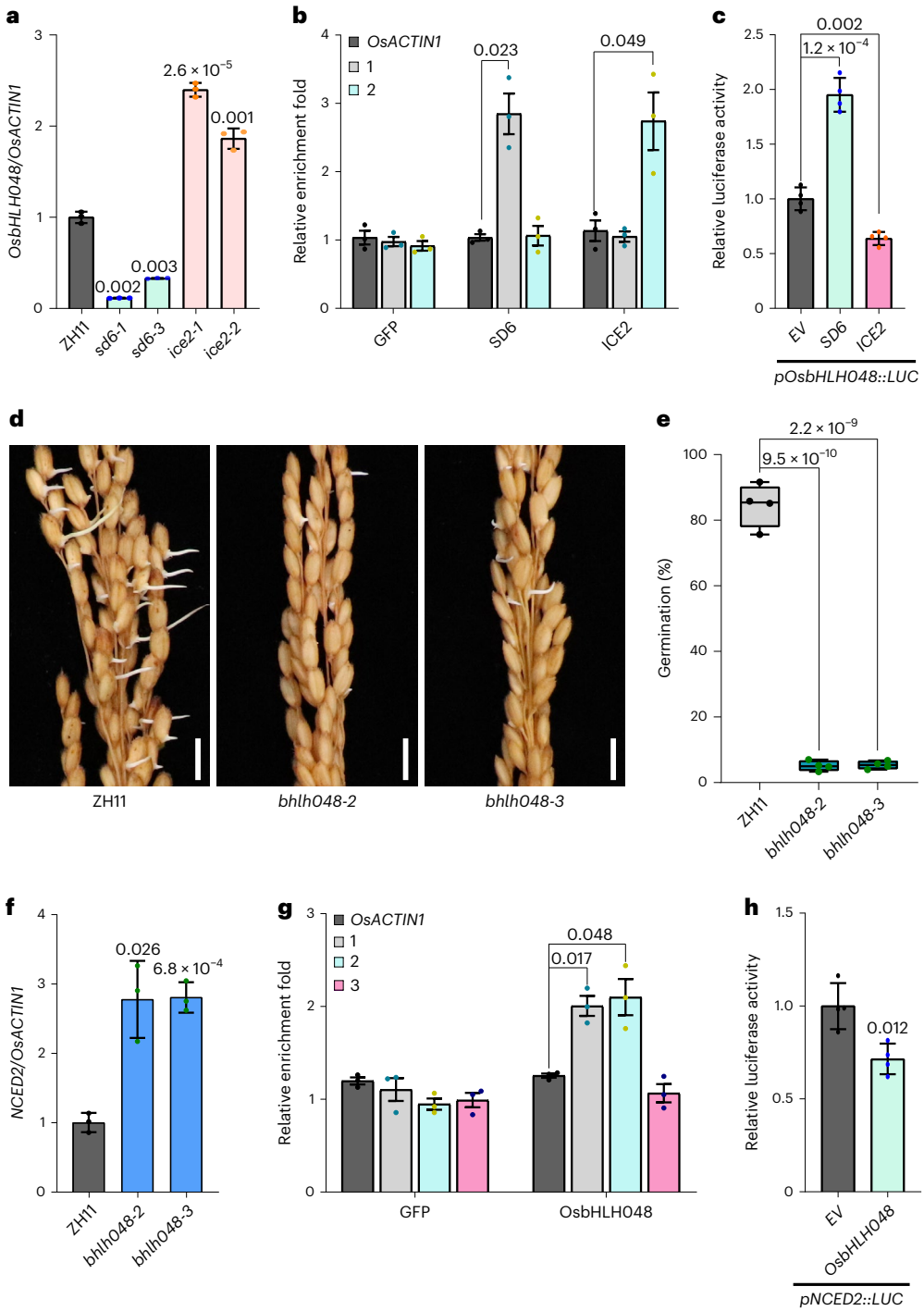

Fig. 4 | *OsbHLH048* attenuates seed dormancy downstream of *SD6* and *ICE2*. **a**, The expression of *OsbHLH048* gene, *LOC_Os02g52190*, in *sd6* and *ice2* mutants. **b**, Relative ChIP-qPCR enrichment of the promoter regions of *OsbHLH048* for SD6 and ICE2. Flag-GFP served as a negative control. Fragment of *OsACTIN1* gene body region was used as interval negative control. 1 and 2 indicate the amplicons of the promoter regions of *OsbHLH048* with G-box (CACGTG) and E-box (CANNTG) motifs, respectively. **c**, *OsbHLH048-LUC* expression in rice protoplasts cotransformed with *SD6* or *ICE2*. **d**,**e**, Germination performance (**d**) and germination percentage (**e**) of seeds in freshly harvested 31–35 DAP panicles of *osbhlh048* mutants. Scale bar, 1 cm. Box plots denote median (horizontal line) with minimum to maximum whiskers. **f**, The expression of *NCED2* in *osbhlh048* mutants. **g**, Relative ChIP-qPCR enrichment of the promoter regions of *NCED2* for OsbHLH048. GFP served as a negative control. Fragment of *OsACTIN1* gene body region was used as interval negative control. One to three represent amplicons of *NCED2* assayed for OsbHLH048 binding as shown in Fig. 3d. **h**, *NCED2-LUC* expression in rice protoplasts cotransformed with *OsbHLH048*. Analysis in **a**–**c**, **f** and **g** was repeated with three biological replicates, and *LUC* expression in **h** was repeated with four biological replicates. Germination test in **d** and **e** was repeated with four panicle replicates and photographs were taken after 7-d imbibition. Data are presented as mean ± s.d. All *P* values are based on two-tailed Student's *t* tests; number marked for each data is the exact *P* value.

SD6 around 24 h imbibition at room temperature, and was significantly suppressed after 12 h imbibition at low temperature when *ICE2* was upregulated (Fig. 5a,b,d).

Only the seeds of *SD6*-overexpressing lines and *ice2* mutants germinated at low temperature as their low temperature-inhibited germination cascades were disturbed (Fig. 5e). To confirm these results,

https://doi.org/10.1038/s41588-022-01240-7

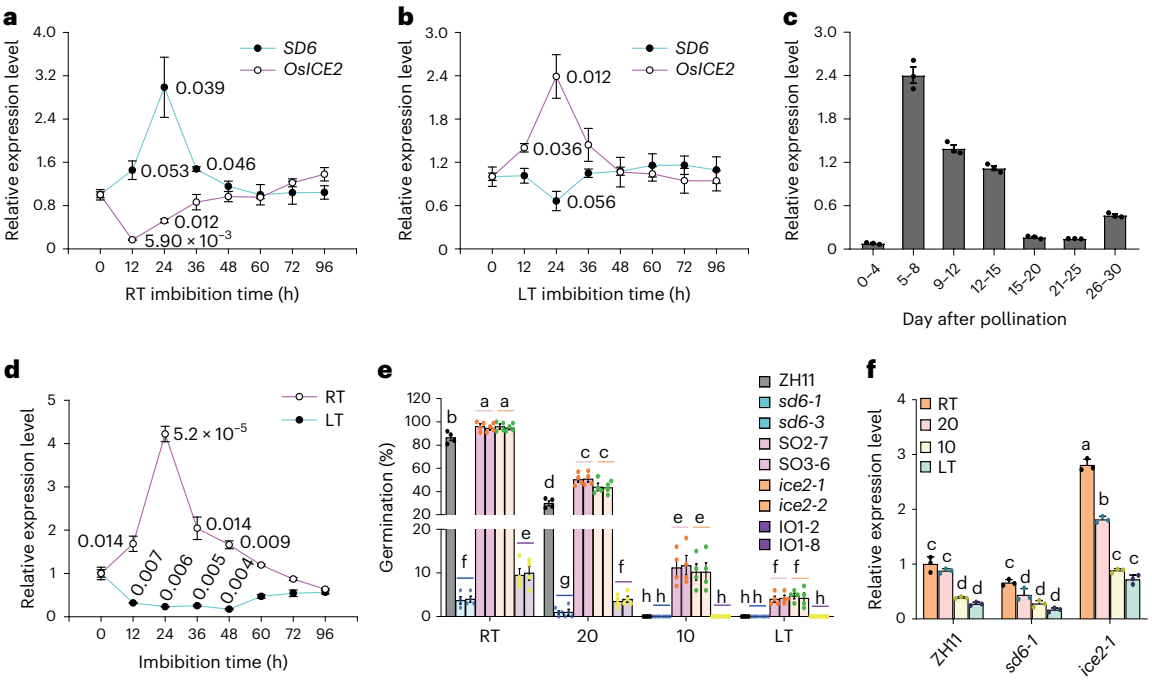

Fig. 5 | The temperature response of *SD6* and *ICE2*. **a**,**b**, The expression level of *SD6* and *ICE2* during germination at room temperature (25 °C) (**a**) and low temperature (4 °C) (**b**). **c**, The expression patterns of *ABA8OX3* in seeds. **d**, The expression level of *ABA8OX3* during germination at room temperature and low temperature. **e**, Germination percentage of seeds in freshly harvested mature panicles of *sd6* and *ice2* mutants and *SD6*- and *ICE2*- overexpression lines at room temperature, 20 °C, 10 °C and low temperature after 1-week imbibition. **f**, The expression of *ABA8OX3* in the seeds of ZH11, *sd6* and *ice2* mutants after 24 h imbibition at room temperature, 20 °C, 10 °C and low temperature. qPCR analysis in **a**–**d** and **f** was repeated with three biological replicates. Germination test in **e** was repeated with four biological replicates. All *P* values in **a**, **b** and **d** indicate significant differences compared to 0-h imbibition by two-tailed Student's *t* test; number marked for each data is the exact *P* value. The data in **e** and **f** were analyzed by two-way ANOVA comparison. Different letters above the bars indicate a significant difference at $P < 0.05$.

we measured the germination of either *SD6*- or *ICE2*-knockout and overexpressing lines at room temperature, 20 °C and 10 °C, respectively. At 20 °C, the germination rate of ZH11 seeds was reduced to one-third of that at room temperature, while the germination rate of the *SD6*-overexpressing line and *ice2* mutant seeds was about half of that at room temperature. And only the seeds of the *SD6*-overexpressing lines and *ice2* mutants germinated at 10 °C (Fig. 5e). Additionally, we examined the expression of *ABA8OX3* in the *sd6-1* and *ice2-1* mutants after a 24-h incubation at room temperature, 20 °C and 10 °C. Specifically, in *sd6-1*, *SD6* was knocked out while *ICE2* was properly working and could be increased in expression at low temperature (Fig. 5b). Consequently, the expression of *ABA8OX3* in *sd6-1* was decreased at room temperature compared with wild type, and was further gradually reduced in response to lowering temperatures (Fig. 5f). In *ice2-1*, *SD6* functioned normally but could be suppressed at low temperature (Fig. 5b). Therefore, *ABA8OX3* expression in *ice2-1* was increased at the room temperature and was gradually reduced as the temperature decreased (Fig. 5f). Moreover, *ABA8OX3* expression was always greater in *ice2-1* than that of the ZH11 control at corresponding temperatures (Fig. 5f), which is consistent with their germination performance under the respective conditions (Fig. 5e). These results suggested that *SD6* is upregulated to trigger seed germination when seeds are at room temperature, while the expression of *ICE2* increases to maintain seed dormancy when they are at low temperature.

Allelic distribution of *SD6* in wild and cultivated habitats

We analyzed the nucleotide diversity (π) of *SD6* using the rice HapMap3 dataset that contained 1,529 rice varieties[50]. The gene region of *SD6* (average $\pi = 0.0006$ in wild rice; average $\pi = 0.0005$ in cultivated rice) showed lower nucleotide diversity comparing to its flanking regions (average $\pi = 0.0029$ in wild rice; average $\pi = 0.0022$ in cultivated rice) (Fig. 6a). In addition, the average nucleotide diversity in *SD6* ($\pi = 0.0006$) is about one-fourth of that ($\pi = 0.0024$) under the whole-genome estimation (https://www.ncbi.nlm.nih.gov/pubmed/23034647). These results implied that *SD6* is functionally conserved in both cultivated and wild rice. We further identified eleven major haplotypes in the coding sequence of *SD6* (Fig. 6b) using the 3,000 rice genome data[51,52]. The *SD6* haplotype in *japonica* and *aus* cultivars was dominated by haplotypes I and IV, respectively, whereas all 11 haplotypes were found in *indica* rice (Fig. 6b,c). Thus, like the haplotype diversity of *SD6*, its nucleotide diversity was lower in *japonica* than in *indica* (Supplementary Table 4).

Given that SNP3 acts as a function mutation, we traced the natural history of *SD6* at this site. Firstly, we inferred the ancestral state at SNP3 by genotyping *Oryza punctata*, which is an outgroup species for the *Oryza* AA-genome species complex including Asian wild and domesticated rice[53]. We found that the C allele at SNP3 is ancestral to the AA *Oryza* species. Interestingly, most species in AA-genome species are fixed for the C allele and variations are only observed within the Asian rice species complex including *O. sativa* and *O. rufipogon*. The T allele at SNP3 is dominant in both temperate and tropical *japonica* subgroups, while T and C alleles at SNP3 have a more balanced distribution in *indica* rice, making T allele the most common haplotype in domesticated rice populations (67.5%). In contrast, the T allele at SNP3 is only found in one of the six subgroups of wild rice, Or-F, which is thought to be a recent feral rice[54] (Fig. 6d). The depletion of the T allele at SNP3 in wild rice populations (chi-squared test, $P < 8 \times 10^{-6}$) is unexpected given continuous and extensive gene flow from domesticated rice to wild rice[54]. Therefore, it is likely that the T allele at SNP3, which confers weaker dormancy, is deleterious under wild conditions and is strongly selected against.

https://doi.org/10.1038/s41588-022-01240-7

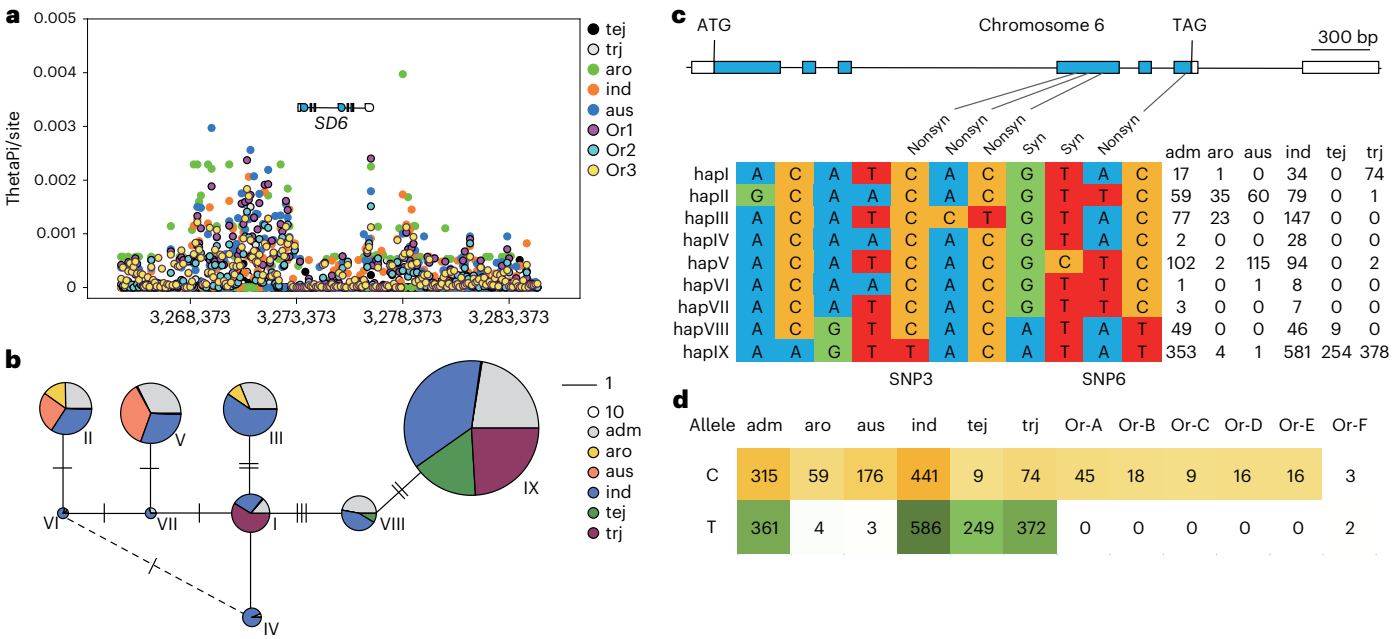

Fig. 6 | Natural variations of *SD6*. **a**, Nucleotide diversity of the *SD6* in cultivated rice and wild rice populations. *y* axis, average ThetaPi/site value; *x* axis, Nipponbare TIGR v7.0 genome coordinate of chromosome 6. **b**, A haplotype network of *SD6*. The haplotype network was constructed based on SNPs at the *SD6* gene region using 3,000 rice genome data. Each pie chart represents one haplotype, and the area of the pie chart is proportional to the haplotype frequency. And each pie chart is further divided based on different rice subgroups within that haplotype. Each segment on the line connecting different pies represents one mutation. The dashed line represents a possible recombination event. **c**, Haplotype analysis of *SD6* using 3,000 rice genome data. **d**, The distribution of SNP3 in various rice subpopulations. tej, *temperate japonica*; trj, *tropic japonica*; ind, *indica*; aus, *Aus*; Or, *O. rufipogon*; Or1, *O. rufipogon* I; Or2, *O. rufipogon* II; Or3, *O. rufipogon* III.

SD6 improves PHS tolerance in rice and wheat

Our results revealed that the *sd6* mutants and NIL-SD6 exhibited strong seed dormancy, and the Nipponbare-type allele of *SD6* is present in more than half of *indica* rice and almost all *japonica* rice, showing a great breeding value of the gene editing of *SD6*. We then generated *sd6* mutants via CRISPR–Cas9 editing in the background of Tianlong619 (T619), Wuyungeng27 (Wu27) and Huaidao5 (Huai5), three high-quality paddy rice cultivars that often suffer from severe PHS. As a result, the field test demonstrated clearly that *SD6* knockout in either T619, Wu27 or Huai5 background effectively prevented the occurrence of PHS (Fig. 7b–e and Extended Data Fig. 9).

In wheat, three bHLH TFs, TraesCS7A02G126900 (TaSD6-A1), TraesCS7B02G026300 (TaSD6-B1) and TraesCS7D02G124700 (TaSD6-D1), have the highest amino acid sequence similarities to SD6 (Extended Data Fig. 10a,b). To confirm the relationship between *TaSD6* and seed dormancy in wheat, we generated triple-recessive biallelic mutants (*aabbdd*) for *TaSD6* in a weak-dormancy wheat cultivar Kenong199 by CRISPR–Cas9 (Extended Data Fig. 10c,d). Interestingly, the triple-recessive homozygous mutants (*tasd6*) showed strong seed dormancy as the rice *sd6* mutants did (Fig. 7f,g and Extended Data Fig. 10e–h). In addition, we also detected significantly increased grain number per spike in *tasd6* mutants (Extended Data Fig. 10i).

Discussion

Dissecting the mechanism of seed dormancy and breeding cultivars with moderate seed dormancy is an important topic in cereal crop breeding. What is really complicated is that seed dormancy represents a type of quantitative domestication trait controlled by multiple genes and affected by various environmental cues. This makes it extremely difficult to identify seed dormancy-related natural variation. Identification of *SDR4* in rice is the only special case[24] and identification of *DOG1* in *Arabidopsis* represents a strategy of combining QTL mapping with mutagenesis screen[55,56]. Cloning of *SD6* is an example of successful application of a mapping strategy that dissects complex traits in rice by first screening of the fixed recombinant individuals (CSSSLs)[57].

SD6 encodes a bHLH type TF, which negatively regulates rice seed dormancy by specifically recognizing the G-box motif in the promoter of an ABA catabolism gene *ABA8OX3* and activates its expression. Moreover, SD6-interacting partner, ICE2, specifically recognizes the E-box motif in the promoter of *ABA8OX3* and represses its expression, resulting in enhanced seed dormancy. We also revealed that there exists SD6/ICE2-OsbHLH048-NCED2 cascade regulating seed dormancy in rice. OsbHLH048 has an opposite function compared to its *Arabidopsis* homolog, AtbHLH57, in regulating seed dormancy in rice. Therefore, our findings reveal a new paradigm for an antagonistic pair of TFs that regulates the biosynthesis and the degradation of a phytohormone at the same time via distinct mechanisms to balance seed dormancy and germination.

In *Arabidopsis*, bHLH TFs, including AtICE1, ZOU and AtbHLH57, are involved in the regulation of seed dormancy[38,58]. AtICE1 and ZOU control primary seed dormancy via enriching the ABI3 promoter and repressing its expression. And *ABI3* is maximally expressed in the developing endosperm and upregulates ABA synthesis, and then suppressing seed germination. Obviously, the mechanism of SD6/ICE2 regulating seed dormancy is different from that of AtICE1/ZOU as we failed to detect a direct transcriptional regulation relationship between SD6/ICE2 and ABI3. In *Arabidopsis*, *ice1* mutant has strong dormancy accompanied by increased ABA level in mature seeds[58]. And the targets of AtICE1, C-repeat binding factors, are associated with temperature sensitivity but absent in imbibed seeds[59]. In rice, ICE1/bHLH002 directly promotes the expression of *OsTPP1*, resulting in enhanced seedling tolerance to chilling[60]. Unlike ICE1, which is preferentially expressed in leaf sheaths, stems, young panicles and ovaries, ICE2 is mainly expressed in endosperm (Extended Data Fig. 8b), suggesting a more specific role of ICE2 in regulating seed dormancy and seed sensitivity to temperature. As many bHLH members are found to be related to seed dormancy,

https://doi.org/10.1038/s41588-022-01240-7

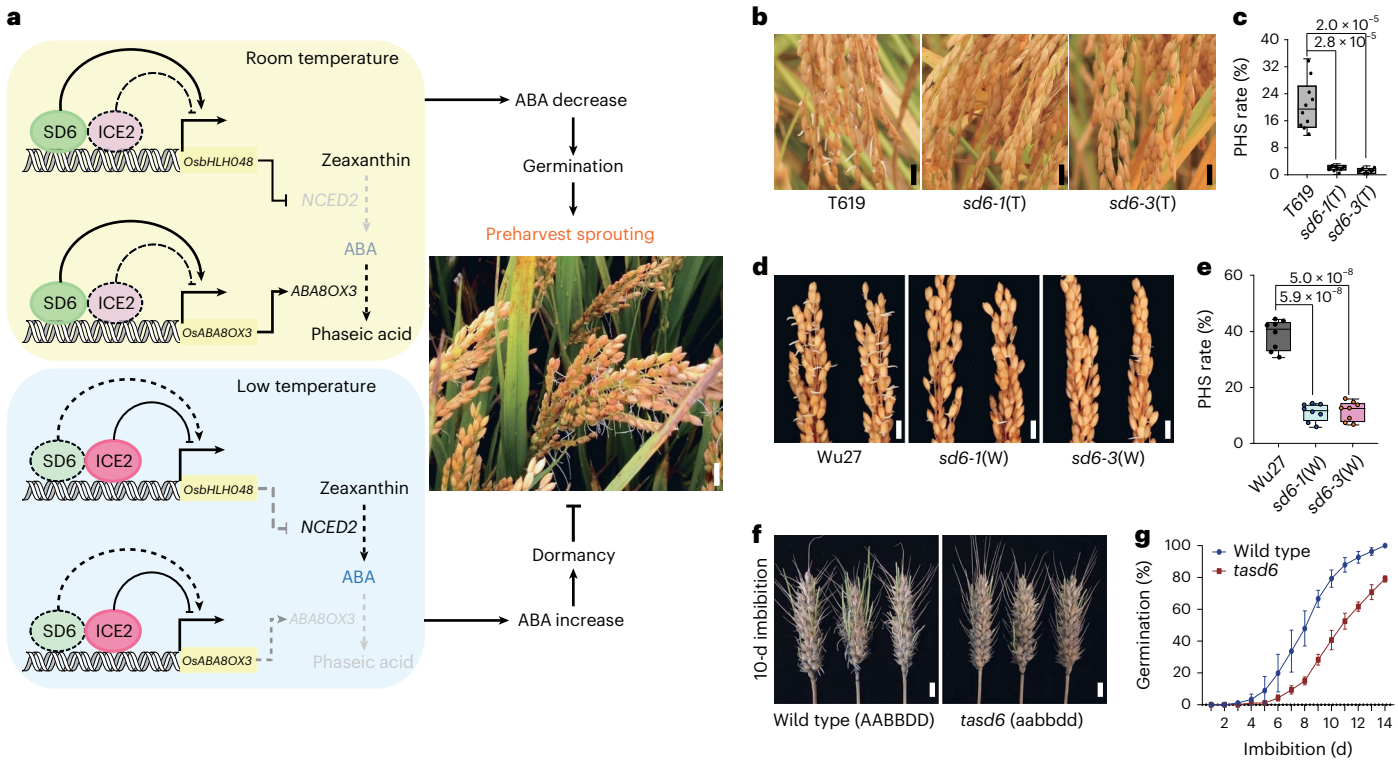

Fig. 7 | Proposed working model and application of *SD6* in rice and wheat. **a**, The proposed working model of SD6 and ICE2. When conditions are suitable for germination (more than 25 °C), *SD6* expression level is significantly elevated, while *ICE2* expression level is sharply reduced, thus promoting the expression of the ABA catabolism gene *ABA8OX3* and also the expression of the *OsbHLH048* gene, which in turn inhibits the expression of the ABA biosynthesis gene *NCED2*. As a result, ABA content is decreased in seeds, which ultimately triggers germination. When seeds are under unsuitable conditions (less than 20 °C), *SD6* expression level is slightly reduced, while *ICE2* expression is elevated, therefore suppressing the expression of the ABA catabolism gene *ABA8OX3*, and also the expression of the *OsbHLH048* gene, which in turn promotes expression of the ABA biosynthesis gene *NCED2*, leading to the increased levels of seed ABA content, and the seeds stay in a dormant state. Scale bar, 2 cm. **b**, The PHS resistance phenotype of *sd6* mutants in T619 background in field conditions for three rainy days. Scale bar, 1 cm. **c**, The PHS rate of *sd6* mutants in T619 after three rainy days. Box plots denote median (horizontal line) with minimum to maximum whiskers. **d**, The PHS resistance phenotype of *sd6* mutants in Wu27 background in field conditions after five rainy days. Scale bar, 1 cm. **e**, The PHS rate of *sd6* mutants in Wu27 after five rainy days. Box plots denote median (horizontal line) with minimum to maximum whiskers. **f**, The PHS resistance phenotype of *sd6* mutants in Kenong199 after 10-d imbibition. Scale bar, 1 cm. **g**, Seed germination rates of wild type and *tasd6* at each day after imbibition. Data are presented as mean ± s.d. Germination test in **c**, **e** and **g** was performed with ten, eight and four panicle replicates, respectively. All *P* values are based on two-tailed Student's *t* tests; number marked for each data is the exact *P* value.

whether other members are also involved in this process and how they cooperate to form a complex regulatory network is worthy of further analysis. Moreover, the coordination between ABA and other phytohormones, especially gibberellin (GA), is critical in regulating seed dormancy[2]. Although we show that SD6, ICE2 and OsbHLH048 form a module to regulate seed dormancy by fine-turning ABA content in rice, whether or how GA level or signaling is affected by them in determining rice seed dormancy remains to be determined.

Temperature is used for temporal sensing to determine the depth of seed dormancy[42,61]. The response to temperature alters the sensitivity of the seeds to their spatial environment signals, including light, nitrate, and water potential, and therefore indicates which condition is suitable for germination[43,62]. *Arabidopsis* seed dormancy increased during winter as soil temperature declined, coinciding with an increase in the expression of ABA synthesis and GA catabolism genes, and also with enhanced transcript level of ABA signaling genes[63]. DOG1 and MFT1 are two important factors determining seed dormancy of *Arabidopsis* soil seed bank in a temperature-dependent manner[63–68]. In rice, our results revealed that SD6 could promote seed germination and ICE2 could deepen seed dormancy in a temperature-dependent manner. When conditions are suitable for germination, *SD6* was significantly elevated, while *ICE2* was obviously downregulated, leading to seed germination. When low temperature is encountered, *SD6* was slightly inhibited and *ICE2* was markedly increased, keeping the seeds in dormancy (Fig. 7a). All these provide an explanation for how seed dormancy works as an adaptive strategy to avoid unsuitable conditions.

Most modern cultivated varieties lack sufficient seed dormancy, resulting in occasional PHS, which causes substantial losses in yield and quality in agricultural production[69]. A useful seed dormancy gene so far is still a scarce resource for effectively improving PHS resistance in crop production under field conditions. *qSD1-2* is allelic to the rice Green Revolution gene *sd1* (ref. [26]) and serious PHS problem in the rice planting regions occurred in recent years under a background that *sd1* has been used to develop high-yield semi-dwarf varieties worldwide since the 1960s. *qSD7-1* is identical to *Rc*, a gene determining seed pericarp color[25]. As white rice is dominant in the global market, it is difficult to use *Rc* to improve seed dormancy on a large scale. In our study, field tests showed that either introduction of natural *SD6* allele to Nipponbare or knockout of *SD6* in elite rice T619, Wu27 and Huai5 could prevent PHS without side effects on other agronomic traits (Supplementary Table 2), indicating that application of *SD6* is a potential strategy for preventing rice PHS in agricultural practice. The large and complex allohexaploid genome of wheat makes it particularly difficult to analyze the complex traits[70]. In addition to several major seed dormancy genes or QTLs such as *TaVP1* and *TaMFT1* have been identified[71–73], we further confirmed that the generation of triple-recessive homozygous mutant

tasd6 is a rapid and useful breeding strategy to enhance seed dormancy in wheat, therefore demonstrating a wide application prospect of *SD6*.

Online content

Any methods, additional references, Nature Portfolio reporting summaries, source data, extended data, supplementary information, acknowledgements, peer review information; details of author contributions and competing interests; and statements of data and code availability are available at https://doi.org/10.1038/s41588-022-01240-7.

References

1. Née, G., Xiang, Y. & Soppe, W. J. J. The release of dormancy, a wake-up call for seeds to germinate. *Curr. Opin. Plant Biol.* **35**, 8–14 (2017).
2. Penfield, S. Seed dormancy and germination. *Curr. Biol.* **27**, R874–R878 (2017).
3. Rodríguez, M., Barrero, J. M., Corbineau, F., Gubler, F. & Benech-Arnold, R. L. Dormancy in cereals (not too much, not so little): about the mechanisms behind this trait. *Seed Sci. Res.* **25**, 99–119 (2015).
4. Lenser, T. & Theissen, G. Molecular mechanisms involved in convergent crop domestication. *Trends Plant Sci.* **18**, 704–714 (2013).
5. Meyer, R. S. & Purugganan, M. D. Evolution of crop species: genetics of domestication and diversification. *Nat. Rev. Genet.* **14**, 840–852 (2013).
6. Wang, M. et al. Parallel selection on a dormancy gene during domestication of crops from multiple families. *Nat. Genet.* **50**, 1435–1441 (2018).
7. Du, L. et al. Endosperm sugar accumulation caused by mutation of *PHS8/ISA1* leads to pre-harvest sprouting in rice. *Plant J.* **95**, 545–556 (2018).
8. Xu, F. et al. Control of rice pre-harvest sprouting by glutaredoxin-mediated abscisic acid signaling. *Plant J.* **100**, 1036–1051 (2019).
9. Zhu, D. W. et al. The effects of field pre-harvest sprouting on the morphological structure and physicochemical properties of rice (*Oryza sativa* L.) starch. *Food Chem.* **278**, 10–16 (2019).
10. Lin, S. Y., Sasaki, T. & Yano, M. Mapping quantitative trait loci controlling seed dormancy and heading date in rice, *Oryza sativa* L., using backcross inbred lines. *Theor. Appl. Genet.* **96**, 997–1003 (1998).
11. Dong, Y. J. et al. Identification of quantitative trait loci associated with pre-harvest sprouting resistance in rice (*Oryza sativa* L.). *Field Crops Res.* **81**, 133–139 (2003).
12. Guo, L. B. et al. QTL analysis of seed dormancy in rice (*Oryza sativa* L.). *Euphytica* **140**, 155–162 (2004).
13. Wan, J. M., Cao, Y. J., Wang, C. M. & Ikehashi, H. Quantitative trait loci associated with seed dormancy in rice. *Crop Sci.* **45**, 712–716 (2005).
14. Wan, J. M. et al. Genetic dissection of the seed dormancy trait in cultivated rice (*Oryza sativa* L.). *Plant Sci.* **170**, 786–792 (2006).
15. Wang, L. et al. Identification of QTLs with additive, epistatic and QTL x development interaction effects for seed dormancy in rice. *Planta* **239**, 411–420 (2014).
16. Cai, H. W. & Morishima, H. Genomic regions affecting seed shattering and seed dormancy in rice. *Theor. Appl. Genet.* **100**, 840–846 (2000).
17. Thomson, M. J. et al. Mapping quantitative trait loci for yield, yield components and morphological traits in an advanced backcross population between *Oryza rufipogon* and the *Oryza sativa* cultivar Jefferson. *Theor. Appl. Genet.* **107**, 479–493 (2003).
18. Lee, S. J., Oh, C. S., Suh, J. P., McCouch, S. R. & Ahn, S. N. Identification of QTL for domestication-related and agronomic traits in an *Oryza sativa* × *O. rufipogon* BC1F7 population. *Plant Breed.* **124**, 209–219 (2005).
19. Li, C. B., Zhou, A. L. & Sang, T. Genetic analysis of rice domestication syndrome with the wild annual species, Oryza nivara. *New Phytol.* **170**, 185–193 (2006).
20. Gu, X. Y., Kianian, S. F. & Foley, M. E. Multiple loci and epistasis control genetic variation for seed dormancy in weedy rice (*Oryza sativa*). *Genetics* **166**, 1503–1516 (2004).
21. Gu, X. Y., Kianian, S. F., Hareland, G. A., Hoffer, B. L. & Foley, M. E. Genetic analysis of adaptive syndromes interrelated with seed dormancy in weedy rice (*Oryza sativa*). *Theor. Appl. Genet.* **110**, 1108–1118 (2005).
22. Gu, X. Y., Kianian, S. F. & Foley, M. E. Isolation of three dormancy QTLs as mendelian factors in rice. *Heredity* **96**, 93–99 (2006).
23. Gu, X. Y., Liu, T. L., Feng, J. H., Suttle, J. C. & Gibbons, J. The *qSD12* underlying gene promotes abscisic acid accumulation in early developing seeds to induce primary dormancy in rice. *Plant Mol. Biol.* **73**, 97–104 (2010).
24. Sugimoto, K. et al. Molecular cloning of *Sdr4*, a regulator involved in seed dormancy and domestication of rice. *Proc. Natl Acad. Sci. USA* **107**, 5792–5797 (2010).
25. Gu, X. Y. et al. Association between seed dormancy and pericarp color is controlled by a pleiotropic gene that regulates abscisic acid and flavonoid synthesis in weedy red rice. *Genetics* **189**, 1515–1524 (2011).
26. Ye, H. et al. Map-based cloning of *qSD1-2* identified a gibberellin synthesis gene regulating the development of endosperm-imposed dormancy in rice. *Plant Physiol.* **169**, 2152–2165 (2015).
27. Wang, Q. et al. OsDOG1L-3 regulates seed dormancy through the abscisic acid pathway in rice. *Plant Sci.* **298**, 110570 (2020).
28. Xie, L. X. et al. Identification and fine mapping of quantitative trait loci for seed vigor in germination and seedling establishment in rice. *J. Integr. Plant Biol.* **56**, 749–759 (2014).
29. Pires, N. & Dolan, L. Origin and diversification of basic-helix-loop-helix proteins in plants. *Mol. Biol. Evol.* **27**, 862–874 (2010).
30. Finkelstein, R., Reeves, W., Ariizumi, T. & Steber, C. Molecular aspects of seed dormancy. *Annu. Rev. Plant Biol.* **59**, 387–415 (2008).
31. Millar, A. A. et al. Seed dormancy and ABA metabolism in *Arabidopsis* and barley: the role of ABA 8′-hydroxylase. *Plant J.* **45**, 942–954 (2006).
32. Okamoto, M. et al. CYP707A1 and CYP707A2, which encode abscisic acid 8′-hydroxylases, are indispensable for proper control of seed dormancy and germination in *Arabidopsis*. *Plant Physiol.* **141**, 97–107 (2006).
33. Finkelstein, R. R., Gampala, S. S. L. & Rock, C. D. Abscisic acid signaling in seeds and seedlings. *Plant Cell* **14**, S15–S45 (2002).
34. Cutler, S. R., Rodriguez, P. L., Finkelstein, R. R. & Abrams, S. R. Abscisic acid: emergence of a core signaling network. *Annu. Rev. Plant Biol.* **61**, 651–679 (2010).
35. Itoh, J. et al. Rice plant development: from zygote to spikelet. *Plant Cell Physiol.* **46**, 23–47 (2005).
36. Chaudhary, J. & Skinner, M. K. E-box and cyclic adenosine monophosphate response elements are both required for follicle-stimulating hormone-induced transferrin promoter activation in Sertoli cells. *Endocrinology* **140**, 1262–1271 (1999).
37. Oh, E. et al. PIL5, a phytochrome-interacting bHLH protein, regulates gibberellin responsiveness by binding directly to the GAI and RGA promoters in *Arabidopsis* seeds. *Plant Cell* **19**, 1192–1208 (2007).
38. Liu, F., Zhang, H., Ding, L., Soppe, W. J. J. & Xiang, Y. REVERSAL OF RDO5 1, a homolog of rice seed dormancy4, interacts with bHLH57 and controls ABA biosynthesis and seed dormancy in *Arabidopsis*. *Plant Cell* **32**, 1933–1948 (2020).
39. Wei, K. & Chen, H. Comparative functional genomics analysis of bHLH gene family in rice, maize and wheat. *BMC Plant Biol.* **18**, 309 (2018).

40. Lu, Y. M. et al. Genome-wide Targeted mutagenesis in rice using the CRISPR/Cas9 system. *Mol. Plant* **10**, 1242–1245 (2017).
41. Li, Q. Q. et al. Synergistic interplay of ABA and BR signal in regulating plant growth and adaptation. *Nat. Plants* **7**, 1108–1118 (2021).
42. Fenner M. (ed.) *Seeds: The Ecology of Regeneration in Plant Communities* (CABI, 2000).
43. Finch-Savage, W. E. & Leubner-Metzger, G. Seed dormancy and the control of germination. *New Phytol.* **171**, 501–523 (2006).
44. Chinnusamy, V. et al. ICE1: a regulator of cold-induced transcriptome and freezing tolerance in *Arabidopsis*. *Genes Dev.* **17**, 1043–1054 (2003).
45. Agarwal, M. et al. A R2R3 type MYB transcription factor is involved in the cold regulation of CBF genes and in acquired freezing tolerance. *J. Biol. Chem.* **281**, 37636–37645 (2006).
46. Miura, K. et al. SIZ1-mediated sumoylation of ICE1 controls CBF3/DREB1A expression and freezing tolerance in *Arabidopsis*. *Plant Cell* **19**, 1403–1414 (2007).
47. Fursova, O. V., Pogorelko, G. V. & Tarasov, V. A. Identification of ICE2, a gene involved in cold acclimation which determines freezing tolerance in *Arabidopsis thaliana*. *Gene* **429**, 98–103 (2009).
48. Zhu, Y., Yang, H. J., Mang, H. G. & Hua, J. A. Induction of BAP1 by a moderate decrease in temperature Is mediated by ICE1 in *Arabidopsis*. *Plant Physiol.* **155**, 580–588 (2011).
49. Kim, Y. S., Lee, M., Lee, J. H., Lee, H. J. & Park, C. M. The unified ICE-CBF pathway provides a transcriptional feedback control of freezing tolerance during cold acclimation in *Arabidopsis*. *Plant Mol. Biol.* **89**, 187–201 (2015).
50. Huang, X. H. et al. Genome-wide association study of flowering time and grain yield traits in a worldwide collection of rice germplasm. *Nat. Genet.* **44**, 32–53 (2012).
51. Mansueto, L. et al. Rice SNP-seek database update: new SNPs, indels, and queries. *Nucleic Acids Res.* **45**, D1075–D1081 (2017).
52. Wang, W. S. et al. Genomic variation in 3,010 diverse accessions of Asian cultivated rice. *Nature* **557**, 43–49 (2018).
53. Wang, M. H. et al. The genome sequence of African rice (*Oryza glaberrima*) and evidence for independent domestication. *Nat. Genet.* **46**, 982–988 (2014).
54. Wang, H. R., Vieira, F. G., Crawford, J. E., Chu, C. C. & Nielsen, R. Asian wild rice is a hybrid swarm with extensive gene flow and feralization from domesticated rice. *Genome Res.* **27**, 1029–1038 (2017).
55. Bentsink, L., Jowett, J., Hanhart, C. J. & Koornneef, M. Cloning of *DOG1*, a quantitative trait locus controlling seed dormancy in *Arabidopsis*. *Proc. Natl Acad. Sci. USA* **103**, 17042–17047 (2006).
56. Bentsink, L. et al. Natural variation for seed dormancy in *Arabidopsis* is regulated by additive genetic and molecular pathways. *Proc. Natl Acad. Sci. USA* **107**, 4264–4269 (2010).
57. Ren, Z. H. et al. A rice quantitative trait locus for salt tolerance encodes a sodium transporter. *Nat. Genet.* **37**, 1141–1146 (2005).
58. MacGregor, D. R. et al. ICE1 and ZOU determine the depth of primary seed dormancy in *Arabidopsis* independently of their role in endosperm development. *Plant J.* **98**, 277–290 (2019).
59. Kendall, S. L. et al. Induction of dormancy in *Arabidopsis* summer annuals requires parallel regulation of *DOG1* and hormone metabolism by low temperature and CBF transcription factors. *Plant Cell* **23**, 2568–2580 (2011).
60. Zhang, Z. Y. et al. OsMAPK3 phosphorylates OsbHLH002/OsICE1 and inhibits its ubiquitination to activate OsTPP1 and enhances rice chilling tolerance. *Dev. Cell* **43**, 731–743 (2017).
61. Finch-Savage, W. E. & Footitt, S. Seed dormancy cycling and the regulation of dormancy mechanisms to time germination in variable field environments. *J. Exp. Bot.* **68**, 843–856 (2017).
62. Batlla, D. & Benech-Arnold, R. L. A framework for the interpretation of temperature effects on dormancy and germination in seed populations showing dormancy. *Seed Sci. Res.* **25**, 147–158 (2015).
63. Footitt, S., Douterelo-Soler, I., Clay, H. & Finch-Savage, W. E. Dormancy cycling in *Arabidopsis* seeds is controlled by seasonally distinct hormone-signaling pathways. *Proc. Natl Acad. Sci. USA* **108**, 20236–20241 (2011).
64. Footitt, S., Huang, Z. Y., Clay, H. A., Mead, A. & Finch-Savage, W. E. Temperature, light and nitrate sensing coordinate *Arabidopsis* seed dormancy cycling, resulting in winter and summer annual phenotypes. *Plant J.* **74**, 1003–1015 (2013).
65. Footitt, S., Clay, H. A., Dent, K. & Finch-Savage, W. E. Environment sensing in spring-dispersed seeds of a winter annual Arabidopsis influences the regulation of dormancy to align germination potential with seasonal changes. *New Phytol.* **202**, 929–939 (2014).
66. Graeber, K. et al. DELAY OF GERMINATION 1 mediates a conserved coat-dormancy mechanism for the temperature- and gibberellin-dependent control of seed germination. *Proc. Natl Acad. Sci. USA* **111**, E3571–E3580 (2014).
67. Chiang, G. C. K. et al. *DOG1* expression is predicted by the seed-maturation environment and contributes to geographical variation in germination in *Arabidopsis thaliana*. *Mol. Ecol.* **20**, 3336–3349 (2011).
68. Footitt, S., Muller, K., Kermode, A. R. & Finch-Savage, W. E. Seed dormancy cycling in *Arabidopsis*: chromatin remodelling and regulation of *DOG1* in response to seasonal environmental signals. *Plant J.* **81**, 413–425 (2015).
69. Hu, W. M., Ma, H. S., Fan, L. J. & Ruan, S. L. Characteristics of pre-harvest sprouting in sterile lines in hybrid rice seeds production. *Acta Agron. Sin.* **29**, 441–446 (2003).
70. Abe, F. et al. Genome-edited triple-recessive mutation alters seed dormancy in wheat. *Cell Rep.* **28**, 1362–1369 (2019).
71. Osa, M. et al. Mapping QTLs for seed dormancy and the *Vp1* homologue on chromosome 3A in wheat. *Theor. Appl. Genet.* **106**, 1491–1496 (2003).
72. Nakamura, S. et al. A wheat homolog of MOTHER OF FT AND TFL1 acts in the regulation of germination. *Plant Cell* **23**, 3215–3229 (2011).
73. Zhou, Y. et al. Genome-wide association study for pre-harvest sprouting resistance in a large germplasm collection of Chinese wheat landraces. *Front. Plant Sci.* **8**, 401 (2017).

Methods

Growth conditions

Oryza sativa L. cv, Nipponbare, Kasalath, ZH11, the chromosome single-segment substitution line (CSSSL) Q27, the nearly isogenic line of *SD6* (NIL-SD6), and the transgenic plants of *SD6*, *ICE2*, *OsbHLH048*, and *ABA8OX3* in ZH11 background were grown in the field of the experimental stations of the Institute of Genetics and Developmental Biology in Beijing (summer) and Lingshui, Hainan province (winter), under natural conditions. *Triticum aestivum* L. cv, Kenong199 and the *tasd6* mutant in the Kenong199 background were grown in the greenhouse of the Institute of Genetics and Developmental Biology in Beijing.

Germination assays

The freshly harvested 31–35 DAP panicles of Nipponbare, Kasalath, ZH11 and the noted transgenic plants were immersed in water. To detect temperature responses in germination, the freshly collected 31–35 DAP panicles of *sd6* mutants and *ice2* mutants were germinated at room temperature (25 °C), 20 °C, 10 °C, and low temperature (4 °C). For each germination assay, at least four panicles were treated. Panicles were transferred to fresh water every day. The number of germinated seeds was counted daily until most of the seeds germinated. The photos are taken after 5-d imbibition. Germination was defined as the coleoptile length reaching to one-half of the grain length. To test the effect of editing *SD6* under natural field condition, T619, Wu27, Huai5 and the corresponding *SD6* knockout plants were cultivated in the experimental fields where continuous rain occurs frequently during the harvest season. About 28 d after heading, the PHS of the plants was monitored every day until the control showed obvious PHS.

Wheat spikes were harvested at 45 DAP, immersed in sterile deionized water, vertically placed on glass vessel and then incubated in a constant temperature incubator at 20 °C. Panicles were transferred to fresh water every day. The photos are taken after 10-d imbibition. In addition, 30 seeds per strain collected at 40 DAP were placed on two layers of filter paper wetted with 8 ml sterile deionized water in a 9-cm Petri dish and incubated in a constant temperature incubator at 20 °C. Seed germination was defined as visible emergence of the coleorhiza beyond the seed coat. To evaluate the dormancy level, the number of germinated seeds was counted daily and used to calculate the germination rate.

For rice materials, germination assays were repeated in Beijing and Hainan for three seasons from 2017 to 2019. For wheat materials, germination assays were repeated in Beijing greenhouse twice in 2020 and in Beijing field once in 2021. And the representative results are presented.

Cloning of *SD6*

Chromosome substitution lines were generated according to the position of seed dormancy QTLs, which were previously reported to be detected stably. For cloning of *SD6*, the CSSSL Q27 was backcrossed with the *japonica* variety Nipponbare to construct the segregation population (BC_6F_2). Fixed homozygous recombinant plants were screened by molecular markers covering the target genomic region. And then the target gene was identified by repeatable phenotypic characterization of these fixed recombinants. The markers developed for genotyping were designed according to the different DNA sequences between *indica* var 9311 and *japonica* var. Nipponbare (http://www.ncbi.nlm.nih.gov). The primer sequences are listed in Supplementary Table 5.

Construction of NIL for *SD6*

From the BC_6F_2 segregation population, we obtained a heterozygote between markers S7 and S4, and then this heterozygote was undergone two generations of self-crossing. We continuously selected target lines in these two generations by markers (Supplementary Table 5) used in genotyping, and finally, identified a NIL for *SD6* carrying an ~20 kb Kasalath segment between markers S7 and S8.

Vector construction and transformation

To knockout *SD6* and *ICE2*, the U3 and U6a primers for *SD6* and *ICE2* were mixed (Supplementary Table 5) to 1 μM, heated at 90 °C for 30 s, and annealed to room temperature, and then inserted into U3 or U6a sgRNA intermediate plasmid at the *Bsa*I site. The gRNA expression cassettes were obtained by two-round PCR using the linkage products as a template, and U-F/gRNA-R primers (first) and B1′/B2 and B2′/BL primers (second); the products were inserted into pYLCRISPR/Cas9-MH binary vectors at *Bsa*I sites to obtain the complete CRISPR/Cas9/sgRNA vectors[74].

To overexpress *SD6* and *ICE2*, the *SD6* and *ICE2* genes were amplified from rice seed cDNA using the SD6OE and ICE2OE primers (Supplementary Table 5), respectively, and homologous recombination was conducted to integrate the sequence into pCAMBIA2300-ACTIN1 (modified from pCAMBIA2300 with the promoter of *OsACTIN1*) using the Infusion HD Cloning Kit (TAKARA, 639648) to construct SD6OE and ICE2OE vectors.

To construct $SD6^{V196A}$OE and $SD6^{S309C}$OE vectors, *SD6* fragments were firstly amplified from rice seed cDNA using the SD6OE-F and T−>C-R, T−>C−F and SD6-R, SD6OE-F and A−>T-R, and A−>T−F and SD6-R, respectively, and then were amplified using the production of first PCR by SD6OE primers and, finally, were homologously recombined to pCAMBIA2300-ACTIN1 (modified from pCAMBIA2300 with the promoter of *OsACTIN1*) using the Infusion HD Cloning Kit.

The *SD6* and *ICE2* genes were amplified from rice seed cDNA using the SD6FLAG and ICE2FLAG primers (Supplementary Table 5), respectively, and were recombined into 1300-Flag (modified from pCAMBIA1300 with Flag) to construct the Flag-SD6 and Flag-ICE2 plasmids.

The plasmids were introduced into rice plants by *Agrobacterium tumefaciens*-mediated transformation[75].

To knockout *SD6* in wheat, the primers of sgSD6 (Supplementary Table 5) were annealed and integrated into the TaU6-sgRNA construct as previously described. Plasmids pJIT163-Ubi-Cas9 and pTaU6-sgSD6 were delivered simultaneously into immature embryos of Kenong199 via particle bombardment, as previously described[76]. After bombardment, the embryos were cultured on a medium without a selective agent to regenerate plantlets. For mutant screening and identification, genomic DNA of pooled leaf pieces from 3 to 4 wheat plantlets was extracted using the high-throughput Automation Workstation Biomek FX (Beckman Coulter). Conserved primers (Supplementary Table 5) were used to identify wheat mutants by PCR amplification and digestion with restriction enzyme Alw44I (PCR-RE assay). Each plantlet in the mutant pools was resampled and tested using A, B and D sub-genome-specific primers (Supplementary Table 5) by PCR-RE assay and Sanger sequencing to identify wheat mutants with indels in target regions.

RNA extraction and quantitative RT-PCR

Total RNA was extracted using an RNA Extraction Kit (BioTek, RP3302). First-strand cDNA was synthesized from 2 μg total RNA using a reverse transcription kit (Toyobo, FSQ301), according to the manufacturer's instructions. Gene-specific primers are listed in Supplementary Table 5. Real-time PCR was performed on the CFX96 Optical Reaction Module (Bio-Rad) using the SYBR qPCR Mix kit (Toyobo, FQPS301), according to the manufacturer's instructions. *OsACTIN1* or *OsUBIQUITIN2* (Ubi) and *TaActin* were used as the internal control, respectively. Each analysis was repeated three times with similar results obtained.

Nucleotide diversity estimation

Sequence data of *SD6* and its 20-kb flanking regions were obtained from the rice HapMap3 of 1,529 varieties[50]. The average nucleotide diversity (ThetaPi/site) of *temperate japonica*, *tropical japonica*, *indica*, *aus* and wild rice *O. rufipogon* subpopulations was estimated in nonoverlapping 100-bp windows using an in-house Perl script; missing data positions were included, with a modification of population size[77]. To construct

the haplotype network of *SD6*, we used the 3,000 rice genome data[51,52]. We first retrieved all the SNPs of the gene region from Asian cultivated rice and then filtered SNPs with a minor allele frequency of less than 5% (11/22 SNPs were filtered). The remaining 11 SNPs form 44 haplotypes. We constructed the haplotype network with 11 major haplotypes whose frequencies are greater than 10 counts using R package pegas[78]. We merged the subgroups from ref. [52] as follows: trp into *tropical japonica* (trj), temp into *temperate japonica* (tej), ind1A, ind1B, ind2, ind3 into *indica* (ind), japx, indx and admix into admixture (adm).

Yeast two-hybrid analysis

The *SD6* and *ICE2* genes were amplified from rice seed cDNA using the SD6AD, SD6BD, ICE2AD and ICE2BD primers (Supplementary Table 5) and recombined into pGADT7 or pGBKT7 to create the SD6AD, SD6BD, ICE2AD and ICE2BD vectors, respectively. Yeast two-hybrid screening and assay were performed according to the manufacturer's instructions for Matchmaker Gold Yeast Two-Hybrid System (TaKaRa, 630490).

Yeast one-hybrid analysis

Sense and antisense oligonucleotides containing a triplication of either the E-box variant or a mutated version were designed. Similarly, sense and antisense oligonucleotides were designed to create a construct containing three copies of G-box or mutated G-box (Supplementary Table 5). Sense and antisense nucleotides were annealed and ligated into the pAbAi plasmid (TaKaRa, 630491) to construct the pAbAi-E-box, pAbAi-mE-box, pAbAi-G-box, pAbAi-mG-box vectors, respectively. The resulting plasmids were transformed into the yeast strain Y1H Gold for stable integration into the yeast chromosome according to the manufacturer's manual of MatchmakerTM Gold Yeast One-Hybrid Library Screening System (TaKaRa, 630491). SD6AD and ICE2AD were transformed into the resulting lines, and interactions were assessed by adding Aureobasidin A according to the manufacturer's manual of MatchmakerTM Gold Yeast One-Hybrid Library Screening System (TaKaRa, 630491).

GST pull-down assays

The *ICE2* gene was amplified from rice seed cDNA using the ICE2GST primers (Supplementary Table 5) and was homologously recombined into pGex-4T-3 to construct the GST-ICE2 vector. The total proteins of Flag-tagged SD6 transgenic plants were extracted by RIPA buffer (50 mM Tris-HCl (pH8.0), 150 mM NaCl, 0.1% SDS, 0.5% Deoxycholate, 1 mM EDTA, 1% Nonidet P40). Pull-down assay was performed using MagneGST Particles following the manufacturer's instructions (Promega, V8870). Pull-down assay was repeated three times with similar results obtained. The mouse monoclonal anti-GST, rabbit polyclonal anti-Flag, HRP-goat anti-mouse and HRP-goat anti-rabbit antibodies used for this study were obtained from HUAXINGBIO with a dilution 1:10,000 (HUAXINGBIO: HX1807, HX1819, HX2032 and HX2032).

Confocal laser scanning microscopy

For subcellular localization, the *SD6*, *ICE2* and *OsbHLH048* genes were amplified from rice seed cDNA using the SD6CeGFP, ICE2RFP and bHLH048GFP primers (Supplementary Table 5), respectively, and homologous recombination was conducted to integrate the sequences into pCAMBIA2300-*35S-eGFP* (C)or pSAT6-mRFP-N1 (C1) using the Infusion HD Cloning Kit to construct SD6-eGFP, RFP-ICE2 and bHLH048-GFP vectors, respectively. The resulting vectors and control vectors were transformed into rice protoplasts as described previously[79].

For the BiFC assays, the *SD6*, and *ICE2* genes were amplified from rice seed cDNA using the SD6SCC and ICE2SCC primers (Supplementary Table 5), respectively, and were recombined into SCYNER and SCYCER to construct the SD6-SCN, SD6-SCC, ICE2-SCN and ICE2-SCC vectors, respectively. The relevant vector couples were cotransformed into rice protoplasts.

Fluorescence signals were detected using confocal laser scanning microscopy (Leica TCS SP5) at 16 h after transformation.

ABA content detection

ABA was extracted from 21–25 DAP seeds of Nipponbare, NIL-SD6, ZH11, and the noted transgenic plants using 2 ml methanol overnight at −20 °C, and the ABA concentration was determined by UPLC–MS/MS (ultra-high performance liquid chromatography–triple quadrupole mass spectrometry)[80]. Each analysis was repeated three times.

Chromatin immunoprecipitation assays

Chromatin immunoprecipitation was performed as described previously with some modification[81]. Briefly, 2-week-old seedlings of Flag-GFP, Flag-SD6, and Flag-ICE2 transgenic lines, and GFP and bHLH048-GFP transient expression rice protoplasts were harvested and were cross-linked with 1% (vol/vol) formaldehyde and then ground to powder in liquid nitrogen. The DNA/protein complex was incubated with micrococcal nuclease (Thermo Scientific) for 3 h, and then immunoprecipitated with anti-Flag (1:100 dilution; HUAXINGBIO, HX1819) or anti-GFP Monoclonal Antibody (GF28R) (1:100 dilution; Thermo Fisher, MA5-15256) antibody using EZ-Magna ChIP A/G Kit according to the manufacturer's instructions (Millipore, 17-10086). After reverse cross-linking and proteinase K treatment, the immunoprecipitated DNA was purified using the Wizard SV Gel and PCR Clean-Up System (Promega, A9282). The prepared DNA in ChIP was quantified by real-time PCR (qRT-PCR) using respective primer pairs (Supplementary Table 5) in a THUNDERBIRD SYBR qPCR Mix with a Bio-Rad CFX96 real-time PCR detection system. The expression levels were normalized to the input sample for enrichment detection as follows: ΔCt (IP) = Ct (IP) − (Ct (Input) − log10 (2)); ΔCt (NoAbs) = Ct (NoAbs) − (Ct (Input) − log10 (2)). The fold enrichment was calculated as $2^{\Delta\Delta Ct}$, where ΔΔCt = ΔCt (NoAbs) - ΔCt (IP). Flag-GFP and GFP served as negative control, respectively. Fragment of *OsACTIN1* gene body region was used as interval negative control. PCR reactions were performed in triplicate for each sample, similar results were obtained in independent experiments.

Transient expression assay

For transient expression assay, the ~2.5 kb promoter regions of *ABA8OX3* and *NCED2*, ~1.9 kb promoter region of *ABA8OX3* that only contained E-box motif and ~3.0 kb promoter region of *bHLH048* were amplified from rice genomic DNA using the primers of ABA8OX3LUC, NCED2LUC, pA8OX3-P2 and bHLH048LUC and were recombined into pGreen0800 to construct the pABA8OX3-LUC, pNCED2-LUC, pA8OX3-P2-LUC and pbHLH048-LUC vectors, respectively. To construct pA8OX3-P1-LUC that contains intact G-box but mutated E-boxes of *ABA8OX3* promoter, the promoter fragments of *ABA8OX3* were firstly amplified from rice genomic DNA using the pA8OX3-P1-1 and pA8OX3-P1-2 primers, respectively. Then the full-length mutated *ABA8OX3* promoter was amplified using the productions of the first PCR by pA8OX3-P1-1F and pA8OX3-P1-2R primers. Finally, PCR products were homologously recombined to pGreen0800 using the Infusion HD Cloning Kit. Transient expression in rice protoplasts was performed as described previously[82]. The pABA8OX3-LUC, pNCED2-LUC, pA8OX3-P1-LUC, pA8OX3-P2-LUC and pbHLH048-LUC constructs were used as reporter, and SD6OE, ICE2OE, $SD6^{V196A}$OE, $SD6^{S309C}$OE and bHLH048-GFP vectors were used as effectors. After transfection, the protoplasts were incubated in the dark overnight. The LUC activity was detected by the Dual-Luciferase Reporter Assay System (Promega, E1960) following the instructions. Renilla LUC activity was used as the internal control. All transient expression assays were repeated with four times with similar results obtained.

Phylogenetic analysis

The amino acid sequences of SD6, ICE2, TaSD6 and their homologs were aligned by MEGA7 software. Phylogenetic trees were constructed with the aligned protein sequences using MEGA7 software with the neighbor-joining method. Bootstrap values were derived from 1,000

replicates[83]. The accession numbers and databases of sequences for constructing these phylogenetic trees can be found in the Data availability section.

Statistics and reproducibility

Numbers (*n*) of samples or replicates are indicated in figure legends and method section. For bar charts, all values are presented as mean ± s.d. For box plots, median with minimum to maximum whiskers are presented. For pairwise comparisons, significance analysis was calculated by two-tailed Student's *t* test using Excel 2013, and the exact *P* values are presented. For multiple-group comparisons, significance analysis was calculated by one/two-way ANOVA as indicated in figure legends using GraphPad Prism 8.0, and are indicated with different letters.

Reporting summary

Further information on research design is available in the Nature Portfolio Reporting Summary linked to this article.

Data availability

Sequence data from this study can be found in the MSU database (http://rice.plantbiology.msu.edu/) under the following accession numbers: *SD6* (LOC_Os06g06900), *ICE2* (LOC_Os01g70310), *NCED2* (LOC_Os12g24800), *ABA8OX3* (LOC_Os09g28390), *OsACTIN1* (LOC_Os03g50885), *OsbHLH048* (LOC_Os02g52190) and *OsUBIQUITIN2* (LOC_Os02g06640). Sequence for constructing the phylogenetic tree of ICE2 (Extended Data Fig. 8) can be found in The *Arabidopsis* Information Resource database (https://www.arabidopsis.org/) or the MSU database (http://rice.plantbiology.msu.edu/) under the following accession numbers: AtICE1 (AT3G26744), AtICE2 (AT1G12860), AtbHLH57 (AT4G01460), ZOU (AT1G49770), SD6 (LOC_Os06g06900), OsICE1 (LOC_Os11g32100), OsICE2 (LOC_Os01g70310), Rc (LOC_Os07g11020), LOC_Os06g44320, LOC_Os03g08930, LOC_Os10g23050, LOC_Os09g29360, LOC_Os02g52190, LOC_Os04g35010, LOC_Os08g38210, LOC_Os01g18870, LOC_Os04g51070, LOC_Os07g36460, LOC_Os02g02820, LOC_Os04g41570, LOC_Os03g56950, LOC_Os04g52770, LOC_Os04g35000, LOC_Os01g13460, LOC_Os03g26210 and LOC_Os07g43530. For Extended Data Fig. 10, HORVU7Hr1G026560 can be found in phytozome v12.1 (https://phytozome-next.jgi.doe.gov/) by selecting the genome of *Hordeum vulgare r1*, and TaSD6-A1 (TraesCS7A02G126900), TaSD6-B1 (TraesCS7B02G026300), TaSD6-D1 (TraesCS7D02G124700), BRADI_1g48400v3, Zm00001d018416, SORBI_3004G336700 and AET7Gv20319600 can be found in EnsemblPlants database (https://plants.ensembl.org/index.html).
Further information and requests for resources and reagents should be directed to and will be fulfilled by C.C. (ccchu@genetics.ac.cn) and C.G. (cxgao@genetics.ac.cn). Source data are provided with this paper.

Code availability

All software used in the study are publicly available on the Internet as described in Methods and Reporting Summary.

References

74. Ma, X. & Liu, Y. G. CRISPR/Cas9-based multiplex genome editing in monocot and dicot plants. *Curr. Protoc. Mol. Biol.* **115**, 31.6.1–31.6.21 (2016).
75. Liu, X. Q., Bai, X. Q., Wang, X. J. & Chu, C. C. OsWRKY71, a rice transcription factor, is involved in rice defense response. *J. Plant Physiol.* **164**, 969–979 (2007).
76. Wang, Y. P. et al. Simultaneous editing of three homoeoalleles in hexaploid bread wheat confers heritable resistance to powdery mildew. *Nat. Biotechnol.* **32**, 947–951 (2014).
77. Thornton, K. Libsequence: a C++ class library for evolutionary genetic analysis. *Bioinformatics* **19**, 2325–2327 (2003).
78. Paradis, E. pegas: an R package for population genetics with an integrated-modular approach. *Bioinformatics* **26**, 419–420 (2010).
79. Zhang, Y. et al. A highly efficient rice green tissue protoplast system for transient gene expression and studying light/chloroplast-related processes. *Plant Methods* **7**, 30 (2011).
80. Fu, J. H., Chu, J. F., Sun, X. H., Wang, J. D. & Yan, C. Y. Simple, rapid, and simultaneous assay of multiple carboxyl containing phytohormones in wounded tomatoes by UPLC–MS/MS using single SPE purification and isotope dilution. *Anal. Sci.* **28**, 1081–1087 (2012).
81. Johnson, L. M., Cao, X. F. & Jacobsen, S. E. Interplay between two epigenetic marks: DNA methylation and histone H3 lysine 9 methylation. *Curr. Biol.* **12**, 1360–1367 (2002).
82. Yoo, S. D., Cho, Y. H. & Sheen, J. *Arabidopsis* mesophyll protoplasts: a versatile cell system for transient gene expression analysis. *Nat. Protoc.* **2**, 1565–1572 (2007).
83. Kumar, S., Stecher, G. & Tamura, K. MEGA7: Molecular Evolutionary Genetics Analysis version 7.0 for bigger datasets. *Mol. Biol. Evol.* **33**, 1870–1874 (2016).

Acknowledgements

We thank Jiayang Li (Institute of Genetics and Developmental Biology, Chinese Academy of Sciences (CAS)) for providing the SCYNER and SCYCER vectors, Yaoguang Liu (College of Life Sciences, South China Agricultural University) for providing the CRISPR–Cas9 vector system. We also thank Zhiming Feng (Yangzhou University) for providing a field photograph of the rice PHS. This work was supported by the grants from G2P project of the Ministry of Science and Technology of China (2020YFE0202300), the Strategic Priority Research Program of CAS (XDA24020000), the Key Research Program of Frontier Sciences, CAS (QYZDJ-SSW-SMC014) and the National Natural Science Foundation of China (32172059).

Author contributions

F.X., J.T. and C.C. conceived the project, designed the experiments and analyzed the data. F.X. and X.C. performed most of the experiments with the help of S.G., S.W. and B.L. who performed the wheat experiments. H.W. and S.O. performed the population genetic analyses. Y.Q. helped create rice mutants. C.C. and C.G. supervised the project. F.X., J.T., S.W., H.W., C.G. and C.C. wrote the manuscript with contributions from all authors.

Competing interests

The authors declare no competing interests.

Additional information

Extended data is available for this paper at https://doi.org/10.1038/s41588-022-01240-7.

Supplementary information The online version contains supplementary material available at https://doi.org/10.1038/s41588-022-01240-7.

Correspondence and requests for materials should be addressed to Caixia Gao or Chengcai Chu.

Peer review information *Nature Genetics* thanks Makoto Matsuoka, Yongzhong Xing, and George W Bassel for their contribution to the peer review of this work.

https://doi.org/10.1038/s41588-022-01240-7

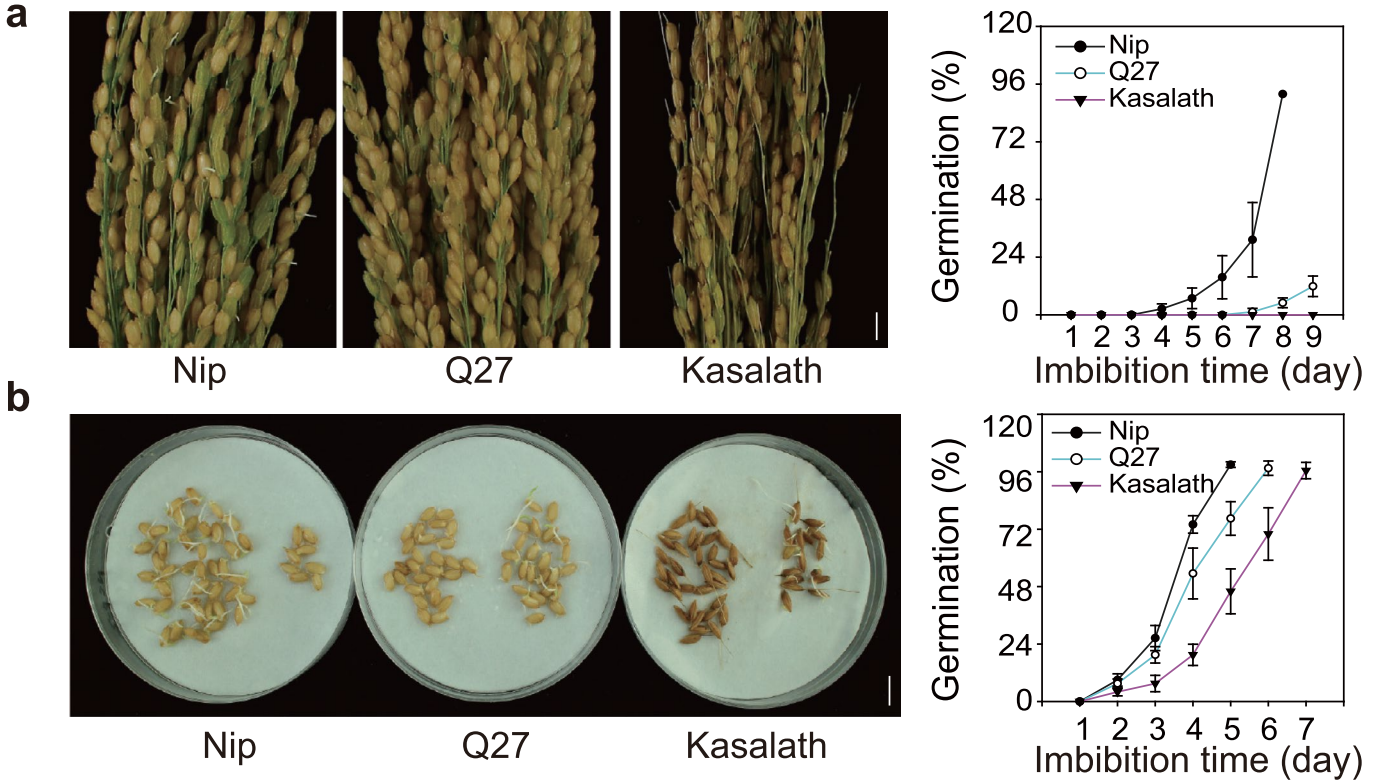

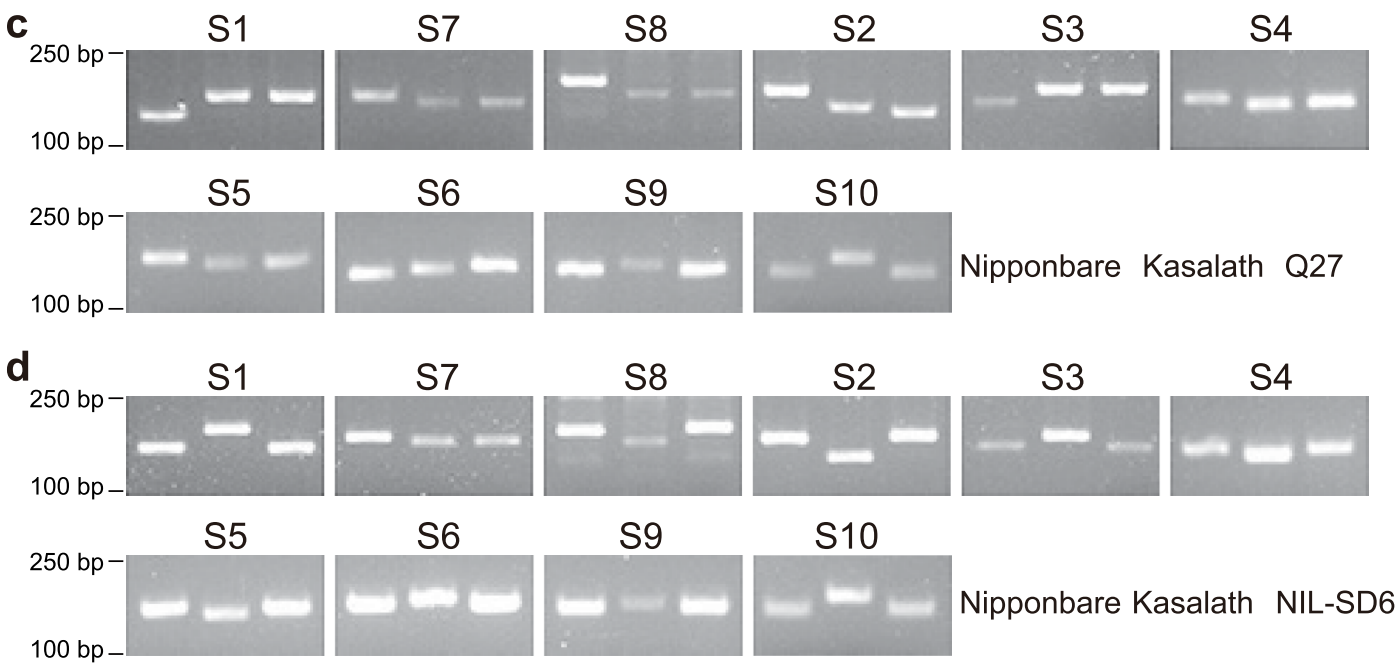

Extended Data Fig. 1 | Characters of CSSSL Q27. a, Germination performance of seeds in freshly harvested CSSSL Q27 panicles. Scale bar 1 cm. Data are presented as mean values ± s.d. Each analysis was repeated with four panicle replicates and photographs were taken after six days imbibition. **b**, Germination performance of breaking dormancy seeds (one week 45°C treatment) of CSSSL Q27. Scale bar 1 cm. Data are presented as mean values ± s.d. Germination test in **b** was repeated with four panicle replicates and photographs were taken after four days imbibition. **c**,**d**, Electrophoretogram of detected fragment of molecular markers S1 to S10 in Q27 (**c**) and NIL-SD6 (**d**). The upper- and lower-boundaries are 100 bp and 250 bp, respectively.

https://doi.org/10.1038/s41588-022-01240-7

Extended Data Fig. 2 | SNP analysis of *SD6*. **a**, SNPs between *SD6*^{Nip} and *SD6*^{Kasa}. **b**, Align of SD6^{Nip} and SD6^{Kasa}. Red, nuclear localization signal (NLS); light blue, basic domain; purple, helix-loop-helix (HLH) domain; yellow, Beta strand.

https://doi.org/10.1038/s41588-022-01240-7

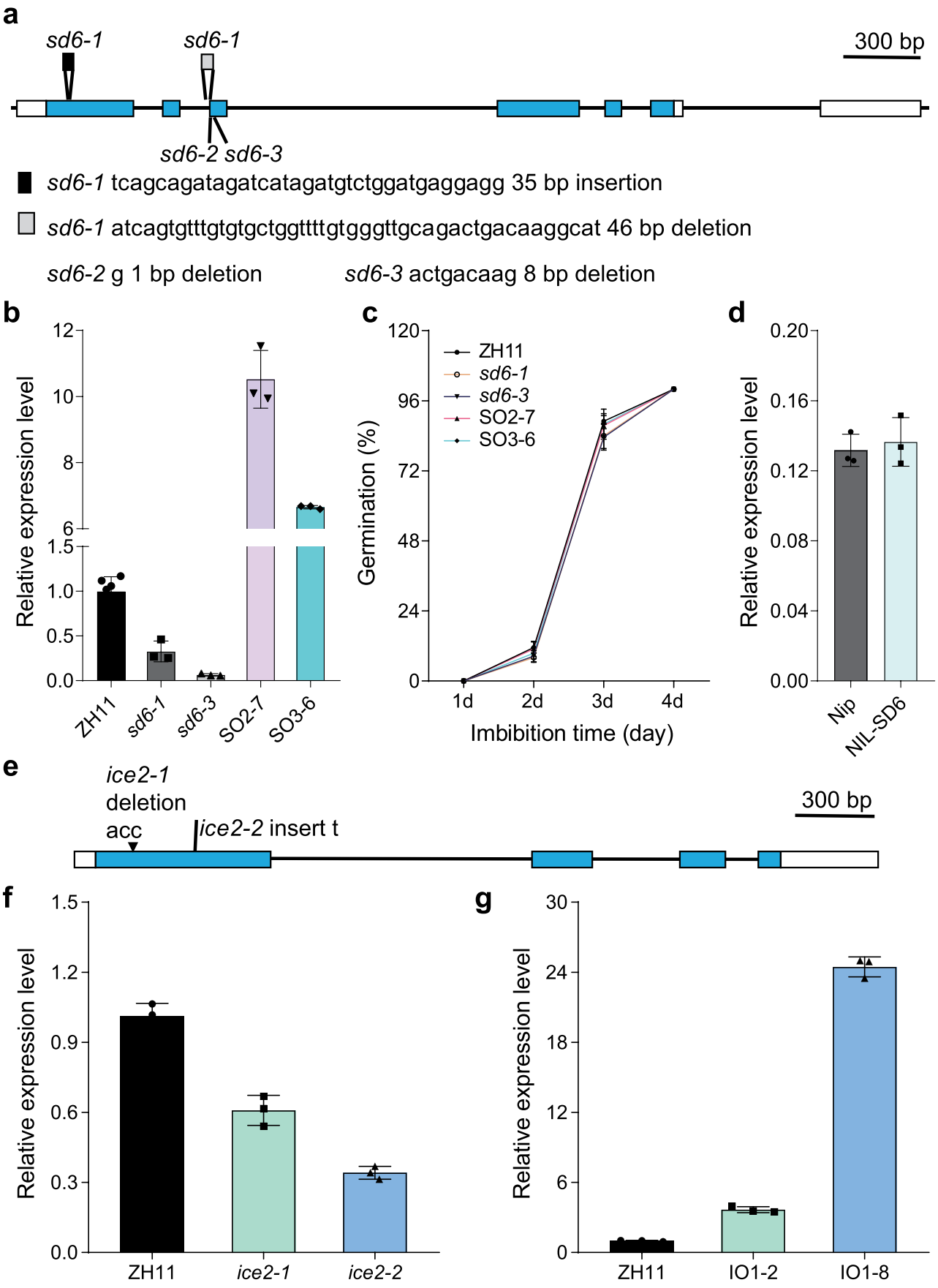

Extended Data Fig. 3 | See next page for caption.

https://doi.org/10.1038/s41588-022-01240-7

Extended Data Fig. 3 | Identification of *sd6* and *ice2* mutants. a, Schematic representation of *SD6* CRISPR-Cas9 mutants. **b**, The expression of *SD6* in *sd6* mutants and *SD6* overexpression plants. **c**, The germination percentage of breaking dormancy seeds (one week 45°C treatment) of *sd6* mutants and *SD6* overexpression plants. **d**, The expression level of *SD6* in Nipponbare and NIL-SD6 seeds detected by qRT-PCR. **e**, Schematic representation of *ICE2* CRISPR-Cas9 mutants. **f**,**g**, The expression of *ICE2* in *ice2* mutants (**f**) and *ICE2* overexpression plants (**g**). Analysis in **b**,**d**,**f**,**g**, was repeated with three biological replicates. Germination test in **c** was repeated with four biological replicates. Data are presented as mean values ± s.d.

https://doi.org/10.1038/s41588-022-01240-7

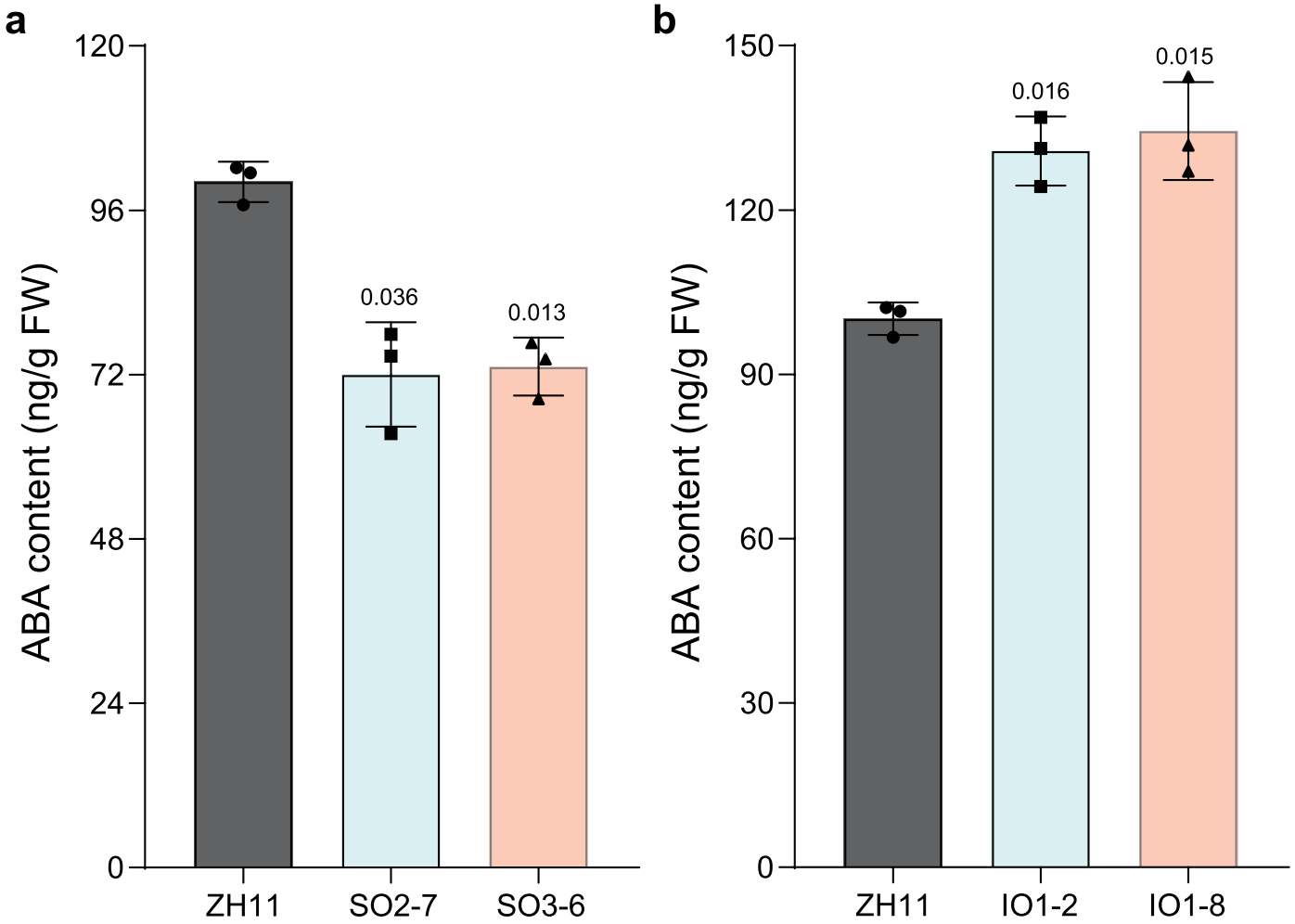

Extended Data Fig. 4 | The ABA content in *SD6*- and *ICE2*-overexpression lines. **a**, The ABA content in freshly harvested 21-25 DAP seeds of *SD6*-overexpression lines (SO2-7 and SO3-6). **b**, The ABA content in freshly harvested 21-25 DAP seeds of *ICE2*-overexpression lines (IO1-2 and IO1-8). Each analysis was repeated with three biological replicates. Data are presented as mean values ± s.d. All *P* values are based on two-tailed Student's *t*-tests.

https://doi.org/10.1038/s41588-022-01240-7

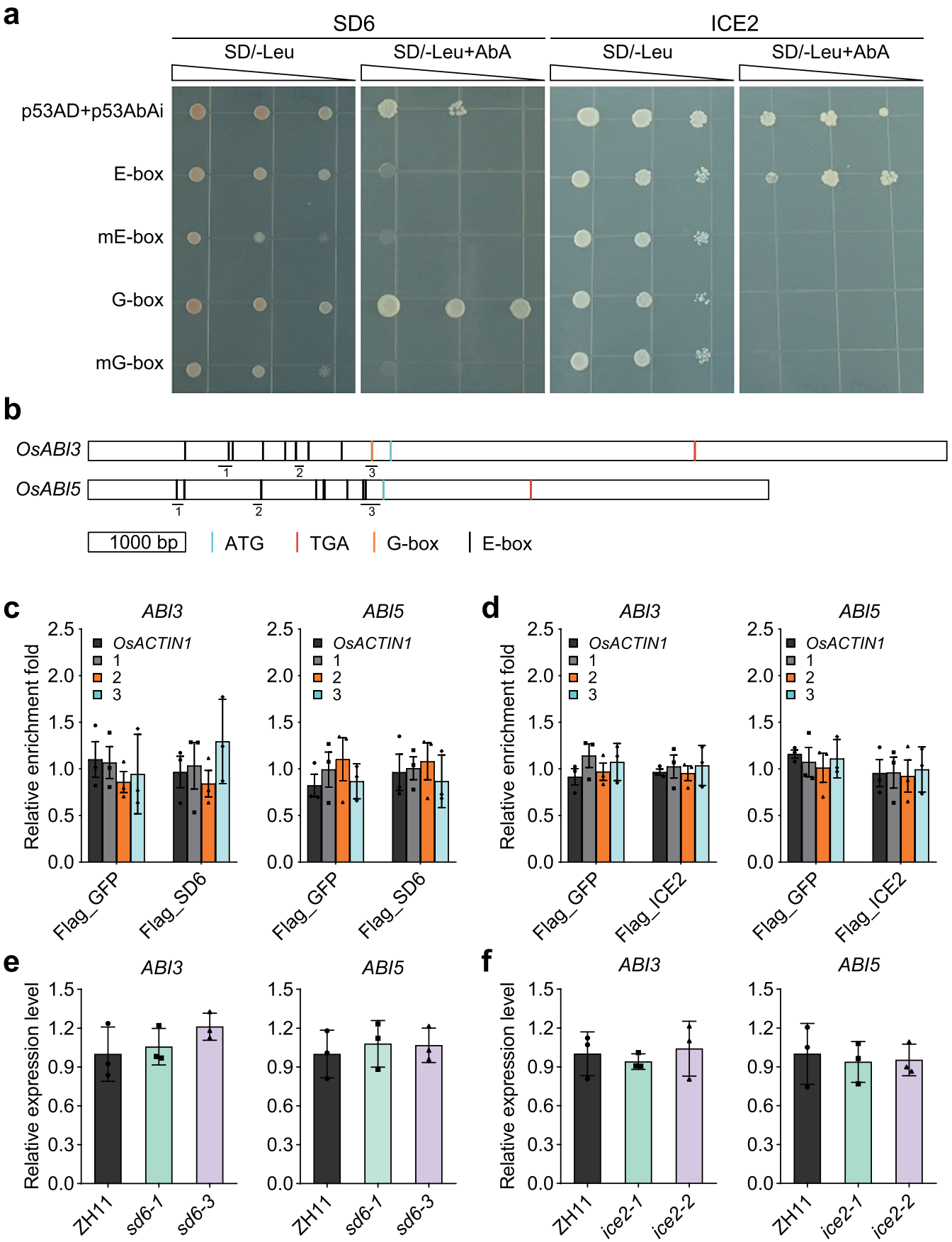

Extended Data Fig. 5 | See next page for caption.

https://doi.org/10.1038/s41588-022-01240-7

Extended Data Fig. 5 | *ABI3* and *ABI5* were not the directly targets of SD6 and ICE2. a, Yeast one-hybrid interactions between SD6 and ICE2 proteins with two elements, 'E-box variant' and 'Triple G-box'. The interaction between p53 proteins and p53 binding elements was used as a positive control, and mutated versions of the E-box and G-box were used as negative controls. **b**, Schematic representation of the indicated genes: Vertical light blue bar represents the start codon ATG; Vertical red bar represents the stop codon TGA; Vertical orange bars represent G-box motifs; vertical gray bars represent E-box motifs; horizontal thin black lines represent amplicons assayed for SD6 and ICE2 binding. **c**,**d**, Relative ChIP-qPCR enrichment of the indicated promoter regions of *ABI3* and *ABI5* for SD6 (**c**) and ICE2 (**d**). Flag-GFP was served as a negative control. Fragment of *ACTIN1* gene body region was used as interval negative control. **e**,**f**, The expression level of *ABI3* and *ABI5* in freshly harvested 21-25 DAP seeds of ZH11, *sd6* mutants, and *ice2* mutants. Each analysis was repeated with three biological replicates. Data are presented as mean values ± s.d.

https://doi.org/10.1038/s41588-022-01240-7

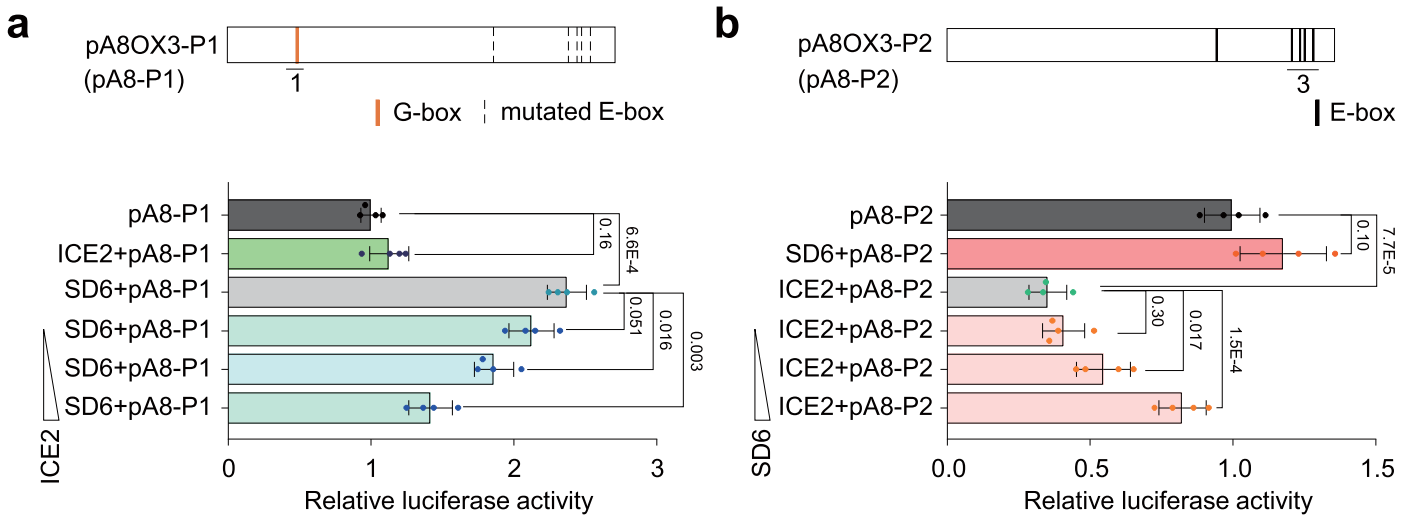

Extended Data Fig. 6 | SD6 and ICE2 mutually impaired their regulation of *ABA8OX3*. **a**,**b**, p*A8*-P1-*LUC* (**a**, only containing G-box motif) and p*A8*-P2-*LUC* (**b**, only containing E-box motif) expression in rice protoplasts co-transformed with $SD6^{Nip}$ and *ICE2*. Each analysis was repeated with four biological replicates. Data are presented as mean values ± s.d. All *P* values are based on two-tailed Student's *t*-tests.

https://doi.org/10.1038/s41588-022-01240-7

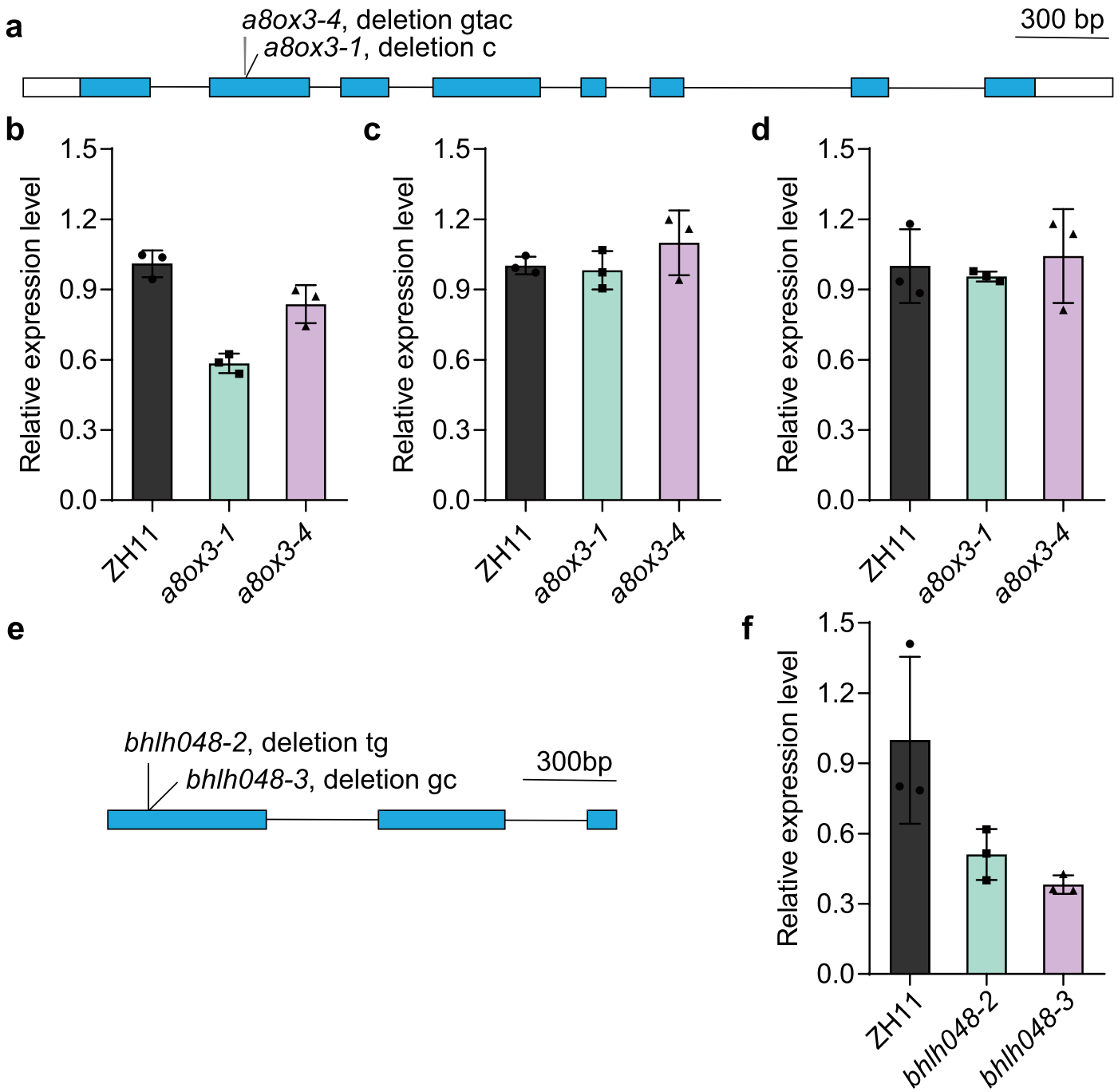

Extended Data Fig. 7 | Identification of *ABA8OX3* and *OsbHLH048* CRISPR-Cas9 mutants. a, Schematic representation of *ABA8OX3* CRISPR-Cas9 mutants. **b**–**d**, The expression of *ABA8OX3* (**b**), *SD6* (**c**), and *ICE2* (**d**) in *aba8ox3* mutants. **e**, Schematic representation of *OsbHLH048* CRISPR-Cas9 mutants. **f**, The expression of *OsbHLH048* in its mutants. Each analysis was repeated with three biological replicates. Data are presented as mean values ± s.d.

https://doi.org/10.1038/s41588-022-01240-7

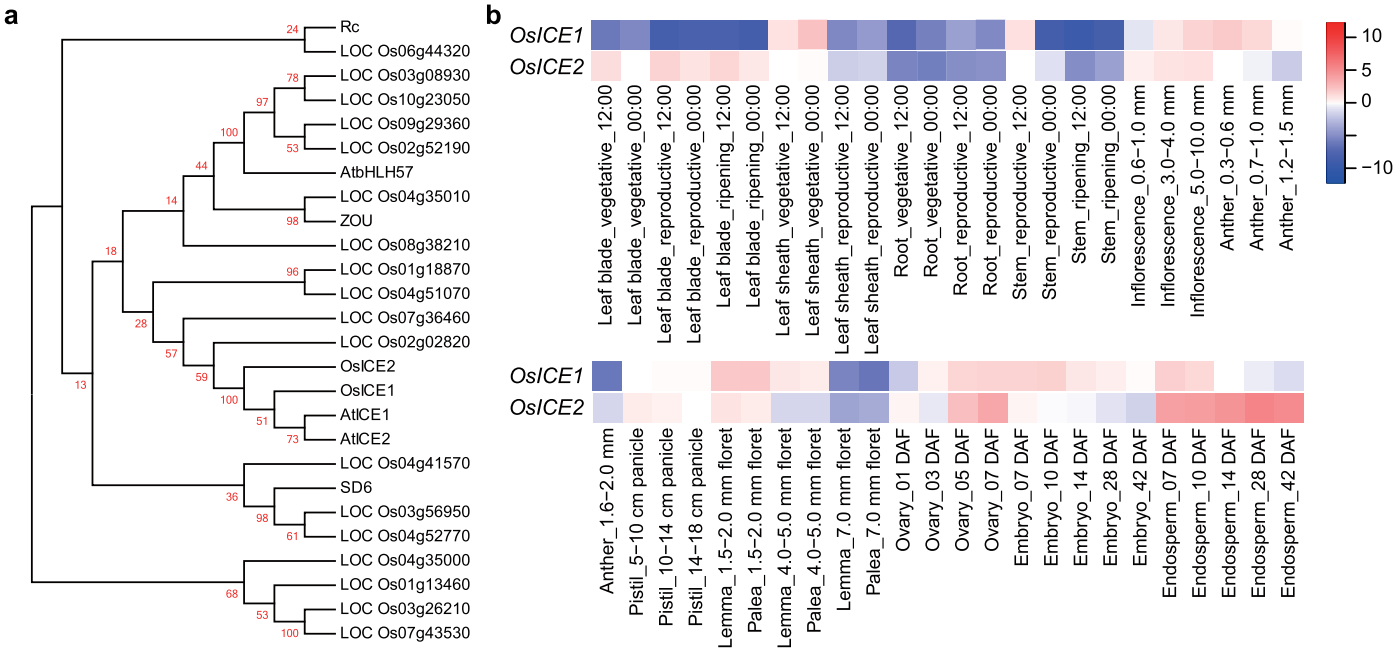

Extended Data Fig. 8 | Phylogenetic analysis of ICE2 and expression profiles of *ICE1* and *ICE2*. **a**, Phylogenetic tree of SD6, ICE2 and its homologous proteins in *Oryza sativa* (ICE1) *Arabidopsis* (AtICE1 and AtICE2), Rc, AtbHLH57 and its homologous proteins in *Oryza sativa*, ZOU, and other bHLHs in rice. **b**, The spatio-temporal expression pattern of *ICE1* and *ICE2* in various tissues/organs throughout entire growth in the field. Data obtained from RiceXPro database (http://ricexpro.dna.affrc.go.jp/).

https://doi.org/10.1038/s41588-022-01240-7

Extended Data Fig. 9 | Germination perfomance of *sd6* mutants in Huaidao5 background. a,**b**, Germination perfomance (**a**) and germination percentage (**b**) of seeds in freshly harvested 31-35 DAP panicles of *sd6* mutants in Huaidao5 (Huai5) background. Each analysis was repeated with four biological replicates and photographs were taken after 5-day imbibition. Scale bar 1 cm. Box plots denote median (horizontal line) with minima to maxima whiskers. All *P* values are based on two-tailed Student's *t*-tests.

https://doi.org/10.1038/s41588-022-01240-7

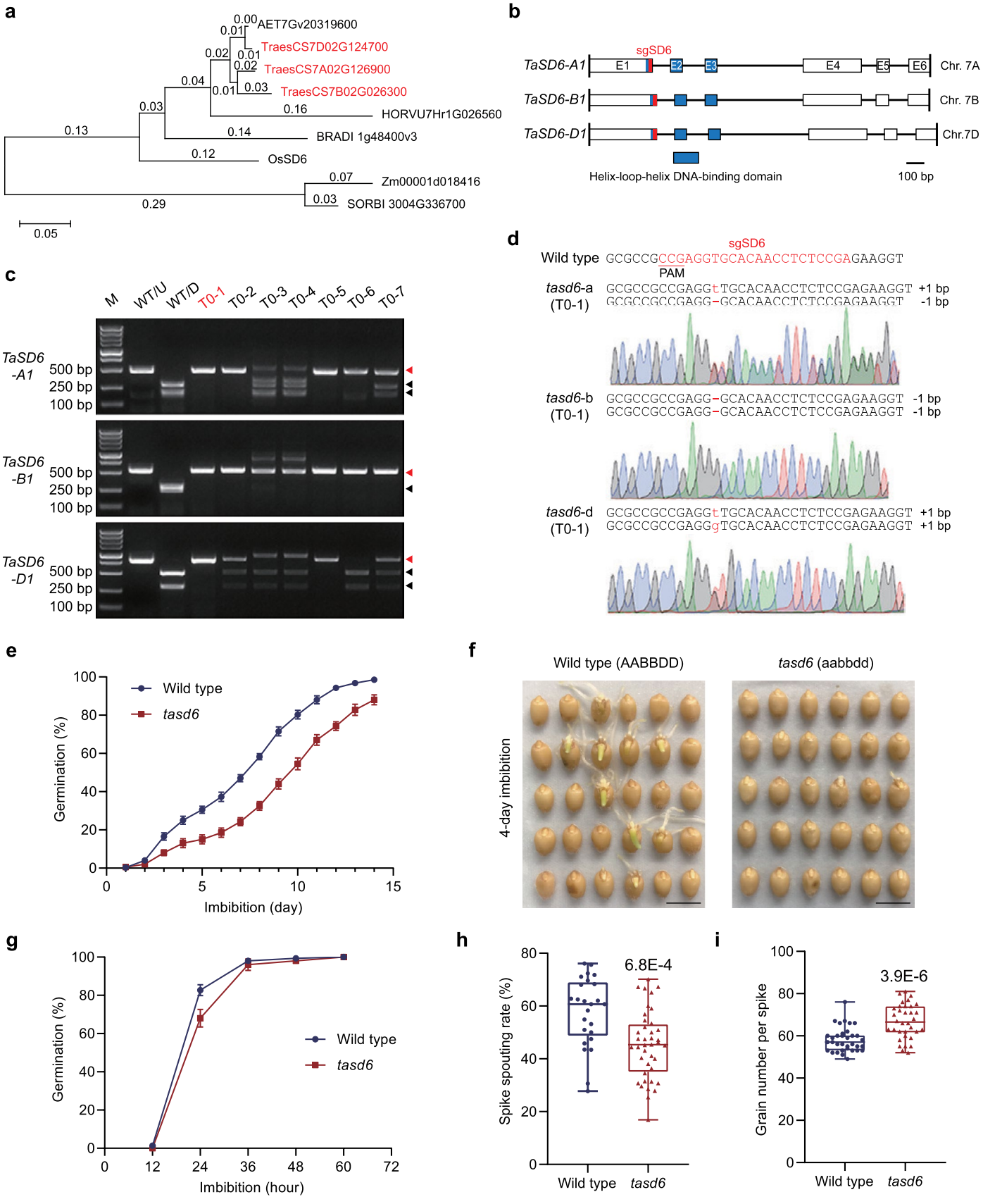

Extended Data Fig. 10 | See next page for caption.

https://doi.org/10.1038/s41588-022-01240-7

Extended Data Fig. 10 | Characters of TaSD6. a, Phylogenetic analysis of SD6 in different cereal crops by the Neighbor-Joining method. Branch lengths represented extents of homology between branches. **b**, Characterization of SD6 homologs in wheat. Exons of *TaSD6* are shown as blue squares, and the target site of CRISPR/Cas9 is marked with red lines in the conserved region encoding the helix-loop-helix DNA-binding domain. **c**, PCR/RE analysis of seven mutants at the target site of *TaSD6*. PCR was performed using A, B, and D sub-genome-specific primers and the products were digested with restriction enzyme Alw44I. **d**, Detailed sequence of the triple-recessive bi-allelic mutant (T0-1) at the target site. The red lowercase letters and short lines represent 1-bp insertions and deletions, respectively. **e**, Seed germination rates of wild type and the triple-recessive homozygous mutant (*tasd6*) at each day after imbibition in 2021. Germination test in **e** was performed with eight biological replicates. Data are presented as mean values ± s.d. **f**, Seed germination status of wild type and the triple-recessive homozygous mutant (*tasd6*) after 4-day imbibition. **g**, Seed germination rates of dormancy-released wild type and *tasd6* via after-ripening at each day after imbibition in 2021. Germination test in **g** was performed with four biological replicates. **h**, Spike spouting rate of wild type and *tasd6* after 6-day imbibition in 2021. Each spike was harvested and incubated under high humidity. **i**, Grain number per spike of wild type and *tasd6*. Analysis in **h** and **i** was repeated with at least twenty-five biological replicates. Scale bar 1 cm. Box plots denote median (horizontal line) with minima to maxima whiskers. All *P* values are based on two-tailed Student's *t*-tests.

nature portfolio

Corresponding author(s): Caixia Gao & Chengcai Chu

Last updated by author(s): Oct 22, 2022

Reporting Summary

Nature Portfolio wishes to improve the reproducibility of the work that we publish. This form provides structure for consistency and transparency in reporting. For further information on Nature Portfolio policies, see our Editorial Policies and the Editorial Policy Checklist.

Statistics

For all statistical analyses, confirm that the following items are present in the figure legend, table legend, main text, or Methods section.

n/a	Confirmed
☐	☒ The exact sample size (*n*) for each experimental group/condition, given as a discrete number and unit of measurement
☐	☒ A statement on whether measurements were taken from distinct samples or whether the same sample was measured repeatedly
☐	☒ The statistical test(s) used AND whether they are one- or two-sided *Only common tests should be described solely by name; describe more complex techniques in the Methods section.*
☒	☐ A description of all covariates tested
☒	☐ A description of any assumptions or corrections, such as tests of normality and adjustment for multiple comparisons
☐	☒ A full description of the statistical parameters including central tendency (e.g. means) or other basic estimates (e.g. regression coefficient) AND variation (e.g. standard deviation) or associated estimates of uncertainty (e.g. confidence intervals)
☐	☒ For null hypothesis testing, the test statistic (e.g. *F*, *t*, *r*) with confidence intervals, effect sizes, degrees of freedom and *P* value noted *Give P values as exact values whenever suitable.*
☒	☐ For Bayesian analysis, information on the choice of priors and Markov chain Monte Carlo settings
☒	☐ For hierarchical and complex designs, identification of the appropriate level for tests and full reporting of outcomes
☒	☐ Estimates of effect sizes (e.g. Cohen's *d*, Pearson's *r*), indicating how they were calculated

Our web collection on statistics for biologists contains articles on many of the points above.

Software and code

Policy information about availability of computer code

Data collection	Sequence data of SD6 and its 20-kb flanking regions were obtained from the rice HapMap3 of 1,529 varieties (Huang et al., 2012). Haplotype network of SD6 was constructed based on the 3,000 rice genome data (Mansueto et al., 2017; Wang et al., 2018). No software was used to collect data.
Data analysis	Microsoft Excel 2013 and GraphPad Prism 8 were used for statistical analysis. The average nucleotide diversity (ThetaPi/site) was estimated using an in-house Perl script (version 1.8.3, Thornton, 2003). R package pegas (version 4.1.3, Paradis, 2010) was used for constructing the haplotype network for SD6. MEGA7 (version 7.0 Kumar, et al., 2016) was used for constructing phylogenetic tree.

For manuscripts utilizing custom algorithms or software that are central to the research but not yet described in published literature, software must be made available to editors and reviewers. We strongly encourage code deposition in a community repository (e.g. GitHub). See the Nature Portfolio guidelines for submitting code & software for further information.

Data

Policy information about availability of data

All manuscripts must include a data availability statement. This statement should provide the following information, where applicable:

- Accession codes, unique identifiers, or web links for publicly available datasets
- A description of any restrictions on data availability
- For clinical datasets or third party data, please ensure that the statement adheres to our policy

Sequence data from this study can be found in the MSU database (http://rice.plantbiology.msu.edu/) under the following accession numbers: SD6 (LOC_Os06g06900), ICE2 (LOC_Os01g70310), NCED2 (LOC_Os12g24800), ABA8OX3 (LOC_Os09g28390), OsACTIN1 (LOC_Os03g50885), OsbHLH048 (LOC_Os02g52190), OsUBIQUITIN2 (LOC_Os02g06640). Sequence for constructing the phylogenetic tree of ICE2 (Extended Data Fig. 8) can be found in The

Arabidopsis Information Resource database (https://www.arabidopsis.org/) or the MSU database (http://rice.plantbiology.msu.edu/) under the following accession numbers: AtICE1 (AT3G26744), AtICE2 (AT1G12860), AtbHLH57 (At4g01460), ZOU (AT1G49770), SD6 (LOC_Os06g06900), OsICE1 (LOC_Os11g32100), OsICE2 (LOC_Os01g70310), Rc (LOC_Os07g11020), LOC_Os06g44320, LOC_Os03g08930, LOC_Os10g23050, LOC_Os09g29360, LOC_Os02g52190, LOC_Os04g35010, LOC_Os08g38210, LOC_Os01g18870, LOC_Os04g51070, LOC_Os07g36460, LOC_Os02g02820, LOC_Os04g41570, LOC_Os03g56950, LOC_Os04g52770, LOC_Os04g35000, LOC_Os01g13460, LOC_Os03g26210, and LOC_Os07g43530. For Extended Data Fig. 10, HORVU7Hr1G026560 can be found in phytozome v12.1 (https://phytozome-next.jgi.doe.gov/) by selecting the genome of Hordeum vulgare r1, and TaSD6-A1 (TraesCS7A02G126900), TaSD6-B1 (TraesCS7B02G026300), TaSD6-D1 (TraesCS7D02G124700), BRADI_1g48400v3, Zm00001d018416, SORBI_3004G336700, and AET7Gv20319600 can be found in EnsemblPlants database (https://plants.ensembl.org/index.html).
Further information and requests for resources and reagents should be directed to and will be fulfilled by Chengcai Chu (ccchu@genetics.ac.cn) and Caixia Gao (cxgao@genetics.ac.cn).

Field-specific reporting

Please select the one below that is the best fit for your research. If you are not sure, read the appropriate sections before making your selection.

☒ Life sciences ☐ Behavioural & social sciences ☐ Ecological, evolutionary & environmental sciences

For a reference copy of the document with all sections, see nature.com/documents/nr-reporting-summary-flat.pdf

Life sciences study design

All studies must disclose on these points even when the disclosure is negative.

Sample size	Samples size for each experiment is indicated in the legends. Required experimental sample size was determined based on experimental trials to allow for confident statistical analyses. Each experiment contains at least three replicates. All replicates represent biologically independent samples. No sample size calculation was performed.
Data exclusions	No data was excluded from the analyses.
Replication	Conclusions drawn in this study are based on at least three independent experiments with similar results. The number of biological replicates in each experiment is indicated in the figure legends.
Randomization	Plants were allocated with different genotypes and were grown side by side to minimize unexpected position effect. Panicles, seeds, or tissues for measurement were randomly sampled from the population of each mutant, overexpression line, and their corresponding controls, respectively.
Blinding	The research materials are plants with different genotypes which should be independently labeled to avoid confusion with each other, making blinding impossible.

Reporting for specific materials, systems and methods

We require information from authors about some types of materials, experimental systems and methods used in many studies. Here, indicate whether each material, system or method listed is relevant to your study. If you are not sure if a list item applies to your research, read the appropriate section before selecting a response.

Materials & experimental systems

n/a	Involved in the study
☐	☒ Antibodies
☐	☒ Eukaryotic cell lines
☒	☐ Palaeontology and archaeology
☒	☐ Animals and other organisms
☒	☐ Human research participants
☒	☐ Clinical data
☒	☐ Dual use research of concern

Methods

n/a	Involved in the study
☒	☐ ChIP-seq
☒	☐ Flow cytometry
☒	☐ MRI-based neuroimaging

Antibodies

Antibodies used

Antibody	Supplier	Catalog number	Dilution
Mouse monoclonal anti-GST	HUAXINGBIO	Cat#HX1807	1:10000
Rabbit monoclonal anti-Flag	HUAXINGBIO	Cat#HX1819	1:10000 for western blot and 1:100 for ChIP-qPCR
HRP-Goat anti-Mouse	HUAXINGBIO	Cat#HX2032	1:10000
HRP-Goat anti-Rabbit	HUAXINGBIO	Cat#HX2031	1:10000
Mouse monoclonal anti-GFP	Thermofisher	MA5-15256	1:100

Validation

The validation for anti-GST, anti-Flag, HRP-Goat anti-Mouse, and HRP-Goat anti-Rabbit can be found at HUAXINGBIO (http://

Validation	www.huaxingbio.com/). The validation for anti-GFP can be found at ThermoFisher (https://www.thermofisher.cn/cn/zh/home.html)

Eukaryotic cell lines

Policy information about cell lines

Cell line source(s)	Yeast (Saccharomyces cerevisiae) strain Y2HGold (TaKaRa, Cat#630498), Y187 (TaKaRa, Cat#630491), and Y1HGold (TaKaRa, Cat#630457)
Authentication	None of the cell lines used were authenticated.
Mycoplasma contamination	The cell lines were not tested for mycoplasma contamination.
Commonly misidentified lines (See ICLAC register)	No commonly misidentified cell lines were used in this study.